Mon. Not. R. Astron. Soc. **353,** 991–1014 (2004) doi:10.1111/j.1365-2966.2004.08130.x

On the highly reddened members in six young galactic star clusters – a multiwavelength study

Brijesh Kumar,[1⋆] Ram Sagar,[1] B. B. Sanwal[1] and M. S. Bessell[2]

[1]*State Observatory, Manora Peak, Nainital, 263 129, Uttaranchal, India*
[2]*Research School of Astronomy and Astrophysics, Mount Stromlo Observatory, Cotter Road, Weston, ACT 2611, Australia*

Accepted 2004 June 16. Received 2004 June 16; in original form 2003 December 16

ABSTRACT

The spectral and reddening properties of 211 highly reddened proper-motion members with $V < 15$ mag in six young galactic star clusters are investigated using low-resolution spectroscopic, broad-band *UBVRIJHK* and mid-infrared (IR) data. We report emission features in Ca II HK and H I lines for a sample of 29 stars including 11 stars reported for the first time and also provide either a new or more reliable spectral class for a sample of 24 stars. Ca II triplet width measurements are used to indicate the presence of an accretion disc for a dozen stars and to indicate luminosity for a couple of stars. On the basis of spectral features, near-IR excesses, dereddened colour–colour diagrams and mid-IR spectral indices we identify a group of 28 pre-main-sequence cluster members including five highly probable Herbig Ae/Be and six classical T Tauri stars. A total of 25 non-emission main-sequence (MS) stars, amounting to ∼10 per cent early-type MS members, appears to show Vega-like characteristics or are precursors to such a phenomenon. The various membership indicators suggest that ∼16 per cent of the proper-motion members are non-members. A significant fraction (>70 per cent) of programme stars in NGC 1976, NGC 2244, NGC 6530 and NGC 6611 show anomalous reddening with $R_V = 4.78 \pm 0.10, 3.54 \pm 0.04, 3.87 \pm 0.05$ and 3.56 ± 0.02, respectively, indicating the presence of grain size dust larger than that typical of the diffuse medium. A small number of stars in NGC 1976, NGC 2244 and NGC 6611 also show normal behaviour while the cluster NGC 6823 appears to have normal reddening. Three highly luminous late-type giants, one in NGC 2244 and two in NGC 6530, appear to be members and are in post-hydrogen-core-burning stages, suggesting a prolonged duration (∼25 Myr) of star formation.

Key words: circumstellar matter – stars: formation – stars: pre-main-sequence – dust, extinction – ISM: general – open clusters and associations: general.

1 INTRODUCTION

The study of differential extinction and the distribution of dust and gas in young clusters (age < 10 Myr) have played an important role in understanding the star-formation processes in them (Elmegreen & Lada 1977; Krelowski & Strobel 1979; Margulis & Lada 1984). The study of the variation of reddening, $E(B - V)$, across the cluster face, with the spectral type and luminosity, indicates that the observed variation of reddening in young open clusters may not be explained by a 'simple' or even 'relatively simple' physical scenario (Sagar 1987). What factors determine the non-uniform extinction in young star clusters and the relatively large value of $E(B - V)$ observed for some members is not understood on the basis of existing observations. Is it the patchiness in the distribution of gas and dust or the circumstellar shells around individual stars or the dust shell around the cluster or is it due to some emission features in the individual members or a combination of any of these?

The early-type stars, being intrinsically luminous and associated with dusty regions, provide invaluable help in probing properties of extinction in the interstellar (He et al. 1995) as well as in the intracluster medium (Sagar & Qian 1993). In order to determine accurate physical properties of young star clusters, extinction contributions from interstellar, intracluster and circumstellar material should be known reasonably well (Pandey et al. 2003). The anomalous extinction behaviour of the interstellar medium is usually characterized by the ratio of the total to selective extinction $R_V = A_V/E(B - V)$, with a normal value of 3.1 for the diffuse dust/clouds (Martin & Whittet 1990; Mathis 1990; He et al. 1995). However, R_V is found to deviate significantly in many directions particularly towards young clusters embedded in dust and gas clouds (Krelowski & Strobel 1987; Pandey et al. 2003, and references therein). In addition to intracluster dust and gas, the anomalous extinction is also

⋆E-mail: brij@upso.ernet.in

caused by the nature of circumstellar material around young stars, for example Herbig Ae/Be, T Tauri and Vega-like stars (Meeus et al. 2001; Hillenbrand 2002; Manoj, Maheswar & Bhatt 2002, and references therein). Moreover the extinction law is found to be uniform in all directions for $\lambda \geqslant 0.9$ μm.

To gain insight into the above questions, systematic spectrophotometric data of highly reddened cluster members are required. Analysis of such data will not only help in studying the role of emission features, if present in these members, but also help in characterizing the intrinsic properties of the star. In general, the previous extinction studies were mainly based on *UBV* data taken primarily with either photographic plates or single-channel photometers in combination with the spectroscopic information derived photometrically. On the other hand, current optical photometry and astrometry, as well as mid-infrared (IR) surveys, allow us to derive multiwavelength information on cluster members. In this paper we present low-dispersion spectroscopic data of a sample of 211 highly reddened proper-motion cluster members mostly in their main-sequence (MS) phase. The brighter members ($V < 15$ mag) with mostly early spectral types are selected from six young galactic clusters. We collected their available *UBVRI* broad-band data from the WEBDA (http://obswww.unige.ch/webda) data base, *JHK* data from 2MASS (2-Micron All Sky Survey – http://www.ipac.caltech.edu/2mass) and mid-IR data from ISOGAL (Infrared Space Observatory GALactic survey – http://www-isogal.iap.fr), MSX (Midcourse Space Experiment – http://www.ipac.caltech.edu/ipac/msx), and *IRAS* (InfraRed Astronomical Satellite – http://vizier.u-strasbg.fr) data bases. Section 2 describes the selection of objects and their observational data for the study, while the results derived from the present analysis and the discussions are presented in the remaining part of the paper.

2 OBSERVATIONS

2.1 Sample selection

Our sample consists of 211 stars in the direction of six young (age < 13 Myr) galactic clusters, namely NGC 1976, NGC 2244, NGC 2264, NGC 6530, NGC 6611 and NGC 6823 (see Table 1). These clusters lie in a highly obscured star-forming regions, viz M42 – OB1 Ori – in Orion, OB2 Mon – Rosette nebula – in Monoceros, OB1 Mon – in Monoceros, M8 – Lagoon nebula – in Sagittarius, M16 – Eagle nebula – in Serpens and OB1 Vul – in Vulpecula, respectively. Their galactocentric distances are in the range 0.4–2.1 kpc. A histogram of the magnitudes of the selected stars is shown in Fig. 1(a). The sample consists of about 72 per cent of early-type

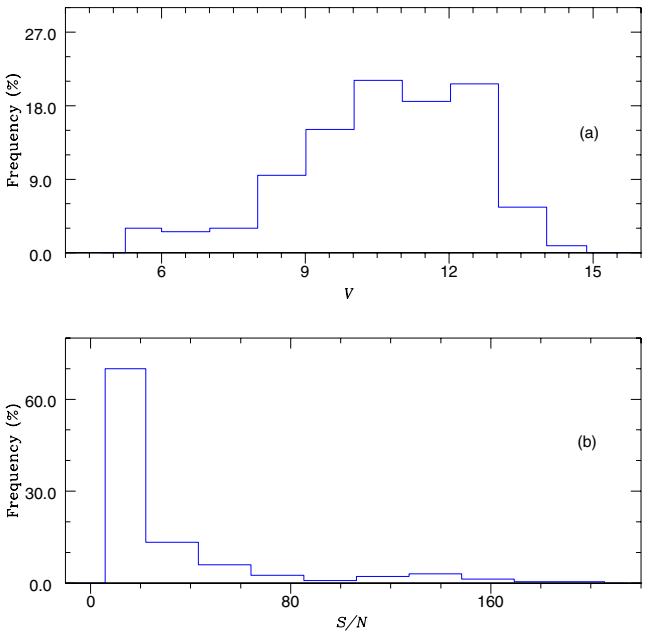

Figure 1. A histogram of signal-to-noise ratio (S/N) and the visual magnitude (V) for the stars under consideration.

stars. There are 22, 109, 20, 20, 24 and 16 cluster members of O, B, A, F, G and K spectral types, respectively. More than 95 per cent of the stars have $E(B-V)$ larger than the mean $E(B-V)$ for their respective cluster. An illustration of the selected stars is shown in a $B-V$ versus $U-B$ diagram for each cluster in Fig. 2. The proper-motion (PM) membership of most of the stars is more than 90 per cent. Around a dozen stars of the sample have either low PM membership probability or belong to the field star population, chosen deliberately to represent interstellar properties in the cluster directions. Thus a large fraction of objects under study are highly reddened PM cluster members. Further details of their spectroscopic and photometric data are described in the following subsections.

2.2 Spectroscopy

The long-slit spectroscopic data were obtained from the Siding Spring Observatory, Australia. The clusters NGC 6530 and NGC 6611 were observed in 1989 August on the Australian National University (ANU) 1-m telescope using a CCD and spectrograph with a dispersion of ∼5.7 Å pixel^{-1} and covering a range of λλ3150–6500. The remaining clusters were observed in 1995 October on the

Table 1. General information on age, distance and mean reddening which are taken from recent studies by Hillenbrand (1997) for NGC 1976, by Massey, Johnson & De Gioia-Eastwood (1995) and Park & Sung (2002) for NGC 2244, by Sung, Bessell & Lee (1997) for NGC 2264, by Sung, Chun & Bessell (2000) for NGC 6530, by Hillenbrand et al. (1993) and Belikov et al. (1999) for NGC 6611 and by Sagar & Joshi (1978), Guetter (1992) and Pigulski, Kołaczkowski & Kopacki (2000) for NGC 6823. The likely age and reddening spread for cluster members are given in columns 2 and 4. Columns 5 and 6 contain cluster samples with $V < 15$ mag and proper-motion probability (p) >50 per cent along with the source of the proper-motion data.

Cluster	Age (Myr)	Distance (kpc)	$E(B-V)$ (mag)	Samples ($p > 50$ per cent)	Source
NGC 1976	1.0(9)	0.47	0.06 (0.02–1.00)	44	McNamara & Huels (1983)
NGC 2244	1.9(6)	1.70	0.47 (0.40–0.56)	43	Marshall, van Altena & Chiu (1982)
NGC 2264	1.5(9)	0.76	0.07 (0.06–1.20)	19	Vasilevskis, Sanders & Balz (1965)
NGC 6530	1.5(5)	1.80	0.35 (0.25–0.50)	45	van Altena & Jones (1972)
NGC 6611	2.0(7)	2.14	0.86 (0.40–1.60)	36	Kamp (1974)
NGC 6823	3.0(9)	2.10	0.85 (0.60–1.16)	24	Erickson (1971)

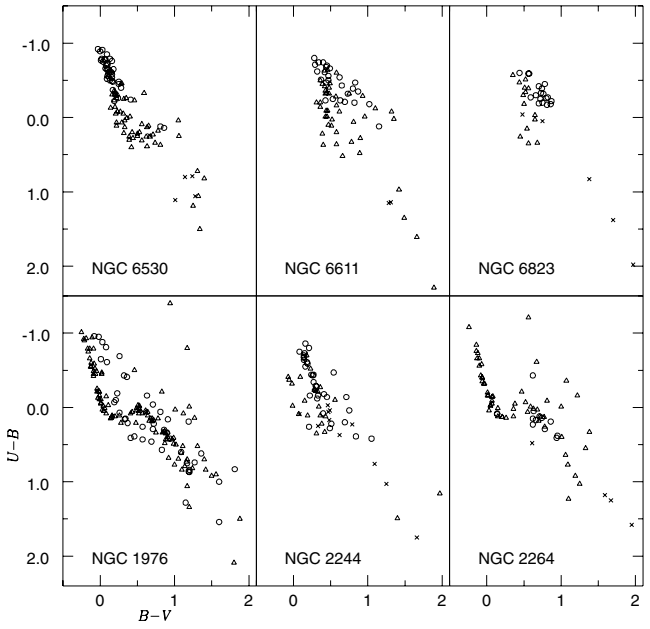

Figure 2. The $B - V$ versus $U - B$ diagram of the cluster members (PM probability >50 per cent and $V < 15$) are shown. The sample stars are shown either with open circles (members) or with crosses (finally rejected from membership). The majority of the selected stars are highly reddened PM cluster members.

ANU 2.3-m telescope using a CCD and the double beam spectrograph with a dispersion of ∼4.0 Å pixel^{-1}, covering the wavelength ranges from 3150 to 6500 Å in the blue and from 5700 to 9800 Å in the red. A sample of 77 stars mostly from NGC 6611 and NGC 6530 therefore have spectra only in the blue region. A consolidated log of observations, spectrographs and grating is given in Tables 2 and 3. Sufficient numbers of bias, flat and arc frames were obtained for calibration purposes. Apart from the cluster stars, several bright and faint spectrophotometric standards were also observed. During the 1995 observations, stars with near blackbody and smooth spectra from tables 3 and 4 of Bessell (1999) were also observed in each night. These are used to remove atmospheric absorption features and any large variations along the spectrum due to detector sensitivity, grating efficiency and spectrograph vignetting.

Data reduction is done using the spectroscopic software packages of IRAF (Image Reduction and Analysis Facility – iraf.noao.edu) and FIGARO (ftp site – ftp.aao.gov.au). Arc frames were used for wavelength calibration. Typical rms uncertainty in wavelength and flux calibrations are 1 Å and 0.05 mag, respectively, for a typical blue region (3500–6500 Å) spectrum with signal-to-noise (S/N) ratio of 20 (see Fig. 1b). Whenever the arc spectra were not taken (see Table 3), the wavelength calibrations were done using Balmer lines of bright A-type standards, which may introduce a further uncertainty in λ calibration of a few angstroms. A set of six flux- and wavelength-calibrated spectra is given in Fig. 3 while the continuum-normalized spectra for all the stars are presented in Fig. 4. This figure is available electronically on *Synergy* and from the authors; only a sample has been presented in the text. The flux is given in AB magnitudes with the zero-point flux of 3.63×10^{-9} erg cm^{-2} s^{-1} Å. In stars 6, 17, 18, 20, 24, 28, 31, 91, 115 and 179, the nebular background was very strong or saturated making for imprecise background subtraction. Seven of these stars belong to the nearest and most fertile star-forming region (i.e. Orion nebula – NGC 1976). The effects of cosmic rays can also be seen in a few spectra (see Fig. 4).

Table 2. Spectrographs, gratings, CCDs and central wavelengths (λ_c). The Boller Chivens Spectrograph (BCS) was used at the ANU 1-m Cassegrain focus and the Double Beam Spectrograph with blue and red arms (DBS-B, R) was used at the ANU 2.3-m Nasmyth focus.

Spect.	Grating	Dispersion		λ_c	CCDs
	(g mm^{-1})	Å mm^{-1}	Å pix^{-1}	(Å)	
BCS	258	260	5.7	4825	GEC (576 × 380, 22μ)
DBS-B	300	140	4.5	4500	SITe(1752 × 532, 15μ)
DBS-R	316	280	4.1	8400	SITe(1752 × 532, 15μ)

The 1995 observations were reduced following the strategies described by Bessell (1999), which has indeed helped us to examine very weak spectral lines of equivalent width (EW) $\leqslant$1 Å such as Na I D, Ca II T and O I T, where D and T stands for doublet and triplet, respectively (see Section 3 for details). The zig-zag continuum can be seen in the blue part of the 1989 spectra while it is absent in 1995 spectra; this effect is more apparent in the normalized spectra (see Fig. 4). The telluric features have not been removed completely for a few stars as they are much dependent on night conditions. In order to check the flux accuracy and correctness of the reduction procedure, the synthetic photometric indices were determined. We found that for 95 per cent of the samples the differences of observed V and $B - V$ with the synthetic ones lying in the range $\pm$ 0.1 mag and $\pm$ 0.05 mag, respectively. The residuals higher than this range may be due to either variability or a low S/N (<10) or a close-by star or emission features or a combination of these. However, we may conclude that the flux accuracy and reduction procedure are correct within observational uncertainties.

2.3 Photometry

2.3.1 Optical

The broad-band Johnson *UBV* and Cousins *RI* data are collected from earlier *UBV* photometry done by us (Sagar & Joshi 1978, 1979, 1981, 1983 for clusters NGC 6530, NGC 6611, NGC 6823 and NGC 2264, respectively) and from the WEBDA data base (Mermilliod & Paunzen 2003, and references therein). For 45 stars, we had only Johnson *RI* data which were converted to the Cousins system using transformations given by Bessell (1979). We could collect simultaneous *UBV* data for all the samples except nine stars which have only *BV* data. There are 83 stars for which we do not have data in either *R* or *I* or in both bands (see Table 4, the full version of which is available on *Synergy*). The maximum uncertainty in the magnitude determination is considered to be ∼0.05 mag. Our sample also contains many known and suspected optical variables (see Table 4). The star 138 is a double star and we consider the brighter component (Walker 1957) in our analysis.

2.3.2 Near-infrared

The near-infrared (NIR) *JHK* data are taken from the ground-based 2MASS Survey (Skrutskie et al. 1997; Cutri 1998), which provides magnitudes for about 471 million point sources observed in the bands J (1.25 μm), H (1.65 μm) and K_s (2.17 μm) with the limiting magnitudes of 15.8, 15.1 and 14.3, respectively. We had *JHK* data available for about 40 per cent of the programme stars in the literature, for example by Qian & Sagar (1994) for NGC 1976,

Table 3. Consolidated log of observations taken with the Siding Spring Observatory (SSO) telescopes.

Date	Tel.	Inst.	Clusters	Obj	Std	Arc
13/14 Aug 1989	1-m	BCS	NGC 6611	36	10	1
13/14 Aug 1989	1-m	BCS	NGC 6530	42	14	–
08/09 Oct 1995	2.3 m	DBS	NGC 2244	12	15	2
09/10 Oct 1995	2.3 m	DBS	NGC 1976, 2244	31	16	1
10/11 Oct 1995	2.3 m	DBS	NGC 1976, 2244, 6823	38	7	–
11/12 Oct 1995	2.3 m	DBS	NGC 6530, 6823	8	1	–
12/13 Oct 1995	2.3 m	DBS	NGC 1976, 2264, 6530, 6823	38	9	–
13/14 Oct 1995	2.3 m	DBS	NGC 1976, 2264	25	4	–

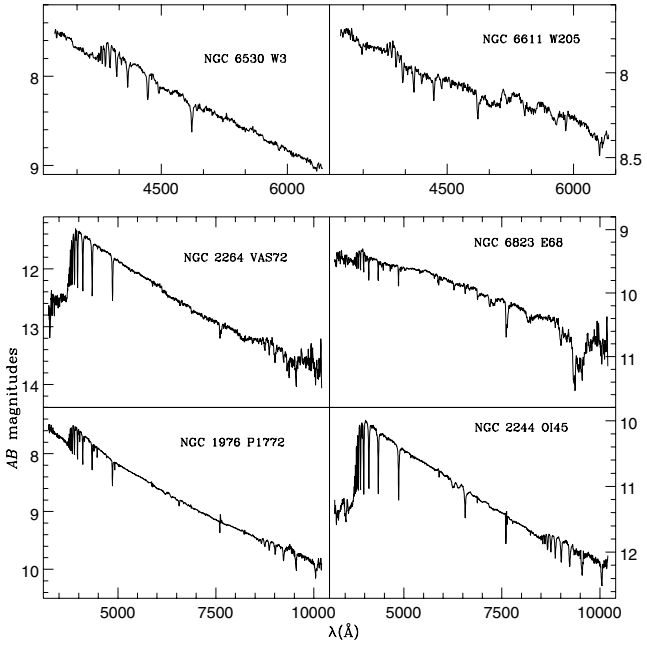

Figure 3. Specimen spectra showing spectral features. The spectral types are determined by means of a cross-correlation technique as described in the text.

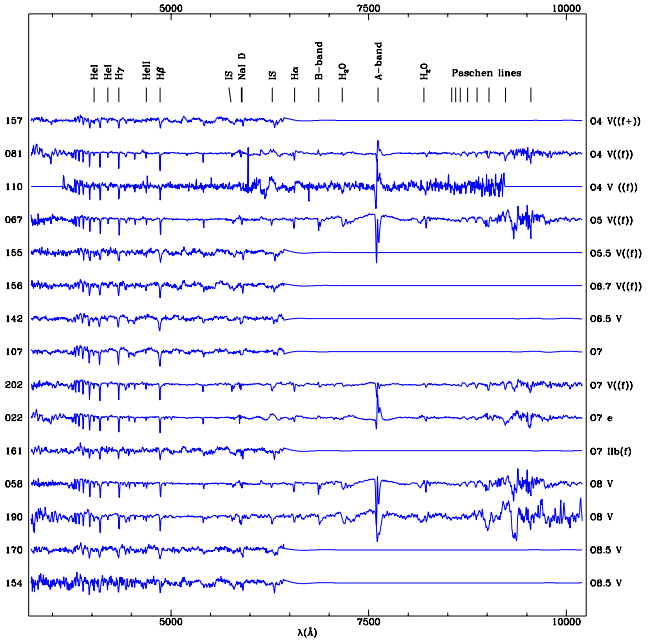

Figure 4. Low-resolution (∼10 Å) spectra in the range 3200–10 200 Å after Fourier filtering of the low-frequency component, arranged in their spectral type sequence. The ID and adopted spectral type are also indicated. The appearance of core emission at Hα for stars 35 and 97 is basically a normalization effect. The red region spectra, if not recorded, as well as the noisy spectra due to low S/N in UV regions are not shown and a solid line is drawn. The spectra between 8900 and 9900 Å are also affected by H_2O bands. The full version of this figure is available in the electronic version of the article on *Synergy* (http://www.blackwellpublishing.com/products/journals/suppmat/mnr/mnr8130/mnr8130sm.htm) as well as from the authors.

Hillenbrand et al. (1993) for NGC 6611 and a few more stars from scattered sources. We collected *JHK* data from 2MASS as it contained homogeneous measurements for most of the sample stars. The K_s magnitude were transformed to the K magnitude using relations given by Carpenter (2001) or the subsequent updates posted on the 2MASS Web site. There are 12 stars for which the quality of the 2MASS data is either poor or the data were not recorded. For six of these stars we took data from the literature, i.e. for stars 17, 18 and 22 from Qian & Sagar (1994); for star 26 from Hillenbrand et al. (1998); for star 56 from Pérez, Thé & Westerlund (1987) and for star 115 from van den Ancker et al. (1997). For the stars 87, 131, 133, 136, 137 and 141 we had either poor S/N (<10) data or had only upper magnitude estimates in the J band. As we had bright NIR sources ($\langle K \rangle \sim 9$ mag) in our samples, almost all stars have a good S/N (>10) ratio. A Gaussian fit to the frequency distribution of uncertainties in the *JHK* bands gives a mean of 0.02, 0.03 and 0.03 mag with a σ of 0.018, 0.022 and 0.022 mag, respectively.

As a further check on the consistency of the NIR data, we compared 2MASS *JHK* magnitudes with those available in the literature for a total of 90, 89 and 91 stars in the J, H and K bands, respectively. The difference in J, H and K magnitude has a mean $\pm$ σ (s.d.) of -0.01 ± 0.08, -0.04 ± 0.11 and -0.05 ± 0.15 respectively. We observed more than 3σ deviation for a total of 16 stars altogether and their numbers are 11, six and seven in J, H and K bands, respectively, out of which only five have the deviation in at least two of the *JHK* bands. Most of these stars have either emission features or show NIR variability (Qian & Sagar 1994; Carpenter 2001). Thus we could secure almost complete broad-band *UBVRIJHK* data for the entire sample of 211 programme stars (see Table 4).

2.3.3 *Mid-infrared*

The mid-infrared (MIR) (7–100 μm) data are taken from the ISOGAL (Omont et al. 2003; Schuller et al. 2003), MSX (Price et al. 2001) and *IRAS* (Beichman et al. 1988) surveys. A total of

Table 4. The first three columns provide identifications. A running number is adopted and is given in column 1. The 'N' in the object column denotes NGC numbers followed by the numbering from Parenago (1954) for NGC 1976 – 'P', from Ogura & Ishida (1981) for NGC 2244 – 'O I', from Vasilevskis et al. (1965) for NGC 2264 – 'VAS', from Walker (1957) or van Altena & Jones (1972) for NGC 6530 – 'W' or 'VA', from Walker (1961) and Kamp (1974) for NGC 6611 – 'W' or 'K' and from Erickson (1971) for NGC 6823 – 'E'. The membership probability (p) is taken from the sources given in Table 1. Spectral type (SpT) as available in the literature with their references given in columns 5 and 6, respectively. Optical and NIR colours are taken from the literature (see text). Further information about asterisked stars and references to SpT are given at the end of the table. The full version of this table is available in the electronic version of the article on *Synergy* (http://www.blackwellpublishing.com/products/journals/suppmat/mnr/mnr8130/mnr8130sm.htm) as well as from the authors.

ID	Object	Others	p (per cent)	SpT	Ref.	$U-V$	$B-V$	V	$V-R$	$V-I$	$V-J$	$V-H$	$V-K$
1*	N1976 P1044	HD 36629	96	B2.5 IV	28	−0.64	0.01	7.69	0.10	–	0.19	0.13	0.17
2	N1976 P1049		61	K2 IV	22	3.14	1.60	11.87	–	–	3.11	3.90	4.11
3*	N1976 P1212	HD 294224	92	B8 V	26	1.15	0.69	11.39	0.49	0.98	1.62	1.87	2.04
4*	N1976 P1360		87	G8 V	32	1.36	0.94	13.81	–	–	1.60	2.03	2.16
5*	N1976 P1409	EZ Ori	94	F8 Vn(e)	32	1.16	0.86	11.57	0.48	0.98	1.90	2.61	3.15

65 stars was found to have associations at least in one band (see Table 5).

ISOGAL provides data mainly in two bands centred around 7 μm, with filters LW2, 6.7 (3.5) μm; LW5, 6.8 (0.5) μm; and LW6, 7.7 (1.5) μm, and around 15 μm, with filters LW3, 14.3 (6.0) μm and LW9, 14.9 (2.0) μm with the detector sensitivity down to 0.01 Jy. We found 28 sources within a search radius of 10 arcsec. Twelve of these stars (169, 175, 190, 191, 192, 195, 197, 198, 200, 204, 203, 107) have a separation of around 5 arcsec while the rest have a separation of around 1 arcsec. We consider these as reliable identifications as the positional accuracy of ISOGAL for DENIS (Deep Near Infrared Survey – http://cdsweb.u-strasbg.fr) associated sources is ∼0.5 arcsec and ∼8 arcsec for non-DENIS associated sources. The stars 190, 191, 192, 195, 196, 197, 198, 200, 203, 204 and 207 were observed in broad-band (LW2, LW3) filters and most of them have fluxes near detector sensitivity (see Table 5). Moreover, most of them are identified within a search radius of ∼5 arcsec. Another 17 stars were observed with narrow-band (LW6 and LW9) filters and were identified within a search radius of ∼1 arcsec. The typical mean uncertainty of these stars is about 0.01 Jy with a quality flag of 4 for most of the associated sources (Schuller et al. 2003).

MSX provides data in four bands, namely A (8.28 μm), C (12.13 μm), D (14.3 μm) and E (21.34 μm), with the highest sensitivity in band A of 0.1 Jy. A total of 23 sources (Table 5) is found to have an MSX counterpart and 12 of these (87, 90, 95, 98, 126, 132, 160, 172, 173, 175, 176, 178) have separations within 2 arcsec while others have a mean separation of 6 arcsec. The typical mean 1σ flux uncertainty for the selected sources is ∼7 per cent, 10 per cent, 11 per cent and 12 per cent, respectively, in the A, C, D and E bands.

IRAS provides fluxes at 12, 25, 60 and 100 μm with a typical detector sensitivity of 0.4, 0.5, 0.6 and 1.0 Jy, respectively. The typical positional uncertainties are ∼25 arcsec. We identified 27 *IRAS* sources to be associated with our programme stars out of which 12 (1, 5, 13, 30, 41, 57, 65, 71, 87, 111, 126, 199) have separations within 30 arcsec while the rest have mean separations of 45 arcsec. Most of these objects are found to have identifiers in the SIMBAD (http://simbad.u-strasbg.fr) data base. However a few of these may be spurious associations considering the positional uncertainties.

Table 5 lists all the stars identified with these catalogues. Nine of these stars (87, 97, 111, 126, 160, 173, 175, 176, 178) have been observed with two surveys. Their fluxes are comparable within observational uncertainty except for stars 111 and 126 where the differences are considerable. This may be either due to wrong association or due to source variability. In many cases, while studying the spectral energy distribution, we considered the average fluxes represented at 7, 12, 15 and 25 μm. For example, the bands of ISOGAl around 7 μm and the A-band fluxes of MSX were averaged to represent the flux at 7 μm.

3 SPECTRAL PROPERTIES

3.1 Spectral classification

A technique based on the cross-correlation method was used to classify the spectra. A set of 161 template spectra having different spectral type and luminosity class was taken from the optical library of Jacoby, Hunter & Christian (1984) but rebinned to the same resolution in the wavelength range 3800–5000 Å as the present data. The continuum of the template as well as programme spectra were approximated by filtering the high-frequency component in Fourier space. The continuum divided (LaSala & Kurtz 1985) spectra were then used for cross-correlation. Each programme star was cross-correlated with the template stars and R-values defined as the ratio of peak height to rms noise (Tonry & Davis 1979) were examined. The spectral type corresponding to the highest R-value was selected. Radial velocity determinations were not attempted as these would have large uncertainties due to low spectral resolution.

A comparison of our spectral types with those in the literature is plotted in Fig. 5. Most of the stars lie within 2 subspectral types while a few of them have larger deviations. This is due to the presence of Balmer line emission in early-type spectra and Ca II HK line emission in late-type spectra. Moreover for late-type stars it may also be due to wrong classification in the literature. In order to confirm the spectral type determined by cross-correlation, we stacked the Fourier filtered spectra, by eliminating high-frequency (noise) and low-frequency (continuum) components, in the sequence of their spectral type (see Fig. 4). This helped us to examine and reclassify the individual spectrum visually using the literature classification as many of the stars have accurately determined spectral types. A large range in spectral types exists in the literature for some, such as star 24 [B0 Vp by Johnson (1965), B8 by Greenstein & Struve (1946), B2 by Levato & Abt (1976)], so we adopt the ones matching with our type. The final adopted spectral type was chosen from the literature, if it was based on higher dispersion, otherwise it is adopted from the present classification. The luminosity class is mostly taken from the literature, if available, otherwise it is considered to be an MS star as per their location in the colour–magnitude and colour–colour diagrams of the respective clusters. However, for a few stars new luminosity classification is also being provided (see Section 3.2). Table 6 lists the finally adopted spectral class including either a new

Table 5. List of programme stars with their ISOGAL, MSX and *IRAS* counterparts. The ISOGAL fluxes at 7 and 15 μm are given along with the MSX fluxes at bands A (∼8 μm) and D (∼15 μm) and *IRAS* fluxes at 12 and 25 μm are given along with the MSX bands C (∼12 μm), D(∼21 μm) so that the common sources can be compared easily. Fluxes are given in janskies (Jy). The *IRAS* fluxes with letter 'L' indicate an upper limit. The last column provides the spectral index (SpI), s ($\lambda F_\lambda \sim \lambda^s$), in the MIR region (2.2–25 μm).

ID	ISOGAL-PJ../IRAS.. MSX5C-G.. (Name)	F7 A (Jy)	F12 C (Jy)	F15 D (Jy)	F25 E (Jy)	F60 (Jy)	F100 (Jy)	SpI (s)
1	05304−0435	–	0.48L	–	4.25	36.45	32.03	−0.42 ± 0.74
5	05318−0506	–	0.46	–	0.55	4.79L	46.55L	−0.79 ± 0.01
13	05327−0529	–	33.86	–	366.60	4798.00	24.48	1.44 ± 0.25
27	05329−0512		22.77	–	54.22L	630.70L	22.69L	0.52 ± 0.10
30	05330−0517	–	82.07	–	560.70	1613.00L	1600.00L	0.85 ± 0.24
36	05333−0543	–	8.52	–	8.07	290.20L	31.41L	0.14 ± 0.37
41	05341−0530	–	3.68	–	7.64	122.30L	648.20L	0.14 ± 0.05
54	06288+0456	–	1.24	–	1.23	2.22L	18.95L	0.72 ± 0.53
57	06288+0452	–	0.71	–	0.63L	2.28L	11.42L	−0.55 ± 0.13
	G206.3519−02.1984	0.42	–	–	–	–	–	
60	06291+0511	–	0.27L	–	2.21	17.54L	16.67L	0.65 ± 0.37
62	06290+0508	–	0.98	–	1.55	2.16L	19.82L	1.24 ± 0.50
65	06289+0504	–	0.30L	–	0.98	2.18L	19.46L	−0.96 ± 0.48
71	06291+0456	–	0.43L	–	0.88	2.47L	20.44L	0.36 ± 0.12
87	06311+0515	–	2.44	–	0.71	2.55	24.10L	−2.55 ± 0.13
	G206.2715−01.5439	3.40	1.74	1.74	–	–	–	
90	06372+0936	–	0.27L	–	0.28L	2.53	15.27L	−2.34 ± 0.48
	G203.1040+01.8224	0.37	–	–	–	–	–	
95	G202.9883+02.0728	0.22	–	–	–	–	–	−2.37
97	06379+0950	–	1.82	–	3.77	1.57L	619.80L	0.30 ± 0.17
	G202.9947+02.1040	1.25	–	1.64	5.14	–	–	
98	G202.9478+02.1479	0.23	–	–	–	–	–	−1.20
101	06382+0939	–	7.06	–	16.25	212.80	499.30	1.54 ± 0.43
109	G005.9186−00.9944	0.83	–	–	–	–	–	0.77
110	18008−2421	–	21.41L	–	32.91	7755.00L	9036.00L	−0.09 ± 0.10
111	18008−2419	–	17.63	–	78.79	347.50L	9036.00L	0.50 ± 0.47
	G006.0569−01.1969	1.20	5.25	6.66	9.83	–	–	
119	G006.1532−01.2200	0.20	–	1.22	2.89	–	–	0.12 ± 0.41
121	18012−2421	–	3.98	–	25.68	26.20L	9036.00L	0.80 ± 0.23
126	18013−2423	–	6.85	–	51.59	429.60L	1184.00L	−0.10 ± 0.58
	G006.0495−01.3286	1.17	2.87	4.34	17.20	–	–	
129	G006.0755−01.3232	0.43	1.76	3.06	10.77	–	–	0.24 ± 0.42
132	G006.0617−01.3519	–	–	–	6.34	–	–	0.44
134	18015−2409	–	2.99	–	3.46	513.50L	1307.00L	−0.08 ± 0.22
146	18006−2422	–	167.70	–	1842.00	7755.00	9036.00	2.80 ± 0.16
149	G006.3342−01.5543	4.03	2.06	1.55	–	–	–	−2.78 ± 0.15
151	G006.4488−01.6002	2.22	–	1.15	–	–	–	−2.79 ± 0.40
152	J181826.2−135005	0.04	–	–	–	–	–	−2.77
153	J181830.0−134957	0.02	–	–	–	–	–	−3.56
154	18156−1343	–	22.78L	–	55.62	1684.00	5317.00	0.59 ± 0.12
155	J181832.7−134512	0.24	–	0.52	–	–	–	−1.70 ± 0.74
156	J181836.1−134736	0.08	–	–	–	–	–	−3.24
157	J181836.4−134802	0.24	–	–	–	–	–	−2.88
160	J181838.8−134644	0.22	–	–	–	–	–	−2.30
	G016.9605+00.8388	0.17	–	–	–	–	–	
161	J181840.1−134518	0.17	–	–	–	–	–	−3.19
166	18159−1346	–	5.97	–	19.30	169.90L	5317.00L	1.46 ± 0.27
167	J181845.9−134631	–	–	0.52	–	–	–	−1.09
169	J181853.2−134939	–	–	0.38	–	–	–	−0.77
170	J181856.2−134830	0.11	–	–	–	–	–	−2.71
171	J181858.7−135928	0.07	–	–	–	–	–	−0.40 ± 1.50
	G016.8149+00.6699	–	–	–	3.38	–	–	
172	G016.8927+00.6807	–	–	1.13	5.06	–	–	0.06 ± 0.38
173	J181904.9−134819	0.22	–	1.26	–	–	–	0.61 ± 0.34
	G016.9870+00.7339	0.34	1.88	2.67	7.89	–	–	
175	J181910.8−135649	0.37	–	0.37	–	–	–	−0.47 ± 0.59
	G016.8754+00.6455	0.41	–	–	3.32	–	–	
176	J181751.1−135055	0.29	–	0.08	–	–	–	−3.00 ± 0.26

Table 5 – *continued*

ID	ISOGAL-PJ../IRAS.. MSX5C-G.. (Name)	F7 A (Jy)	F12 C (Jy)	F15 D (Jy)	F25 E (Jy)	F60 (Jy)	F100 (Jy)	SpI (*s*)
	G016.8083+00.9765	0.17	–	–	–	–	–	
177	J181806.4−133625	0.13	–	–	–	–	–	−3.14
178	J181906.5−135745	0.20	–	–	–	–	–	−2.64
	G016.8516+00.6530	0.27	–	–	–	–	–	
179	J181920.1−135420	0.05	–	0.37	–	–	–	−0.62 ± 0.96
188	19399+2312	–	1.13		2.27	23.31L	80.20L	−0.33 ± 0.09
190	J194211.2+232604	0.10	–	0.02	–	–	–	−2.95 ± 0.07
191	J194222.4+232305	0.01	–	–	–	–	–	−2.84
192	J194227.1+232038	0.01	–	–	–	–	–	−2.67
195	J194249.2+232754	0.16	–	0.03	–	–	–	−2.99 ± 0.09
196	J194254.8+231855	–	–	0.01	–	–	–	−1.62
197	J194306.5+231618	0.03	–	–	–	–	–	−2.93
198	J194309.5+232621	0.03	–	0.01	–	–	–	−2.72 ± 0.12
199	19410+2322	–	0.59	–	0.93	2.26L	43.78L	−1.65 ± 0.39
200	J194310.7+231751	0.08	–	0.02	–	–	–	−1.36 ± 0.63
203	J194312.2+231634	0.02	–	0.05	–	–	–	−1.64 ± 0.79
204	J194313.3+231912	0.02	–	0.02	–	–	–	−1.89 ± 0.24
	G059.4253−00.1490	0.10	–	–	–	–	–	
207	J194316.5+231915	–	–	0.04	–	–	–	−1.30
210	G059.3539−00.2348	0.51	1.35	–	–	–	–	0.16 ± 0.21

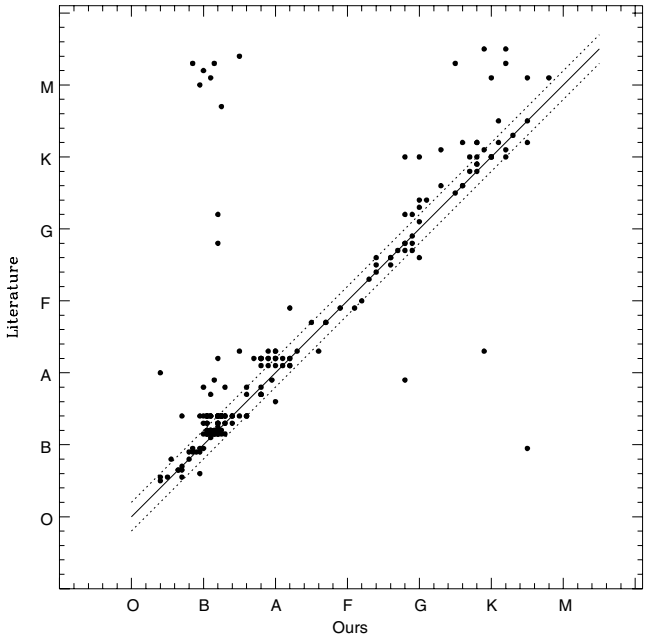

Figure 5. Comparison of the spectral classification as obtained from the cross-correlation method with that available in the literature. The solid line represents a slope of 45° indicating a perfect match while the dotted lines are drawn to denote an uncertainty of two subspectral classes. Points showing large mismatch are discussed in the text. Most of the spectra were reclassified using local standards.

or a more reliable classification for a sample of 24 stars indicated with an asterisk.

3.2 Spectral features – Ca II HK, H I, Ca II T, O I T and Na I D lines

Emission features in the Balmer and Ca II HK lines were reported for a total number of 43 stars on the basis of optical spectra taken mainly in the classical MK region (3800–5000 Å) and/or Hα region (see Table 4 and references therein). We could not confirm the reported emission features for 25 of them. Some of these emission features are in the Hα region where we do not have data for 77 stars and for some stars the reported features are not seen at our resolution or the features may be absent. We confirm the spectral peculiarities for 18 stars reported earlier and find spectral peculiarities for another 11 stars for the first time. The prominent spectral peculiarities for all these 29 stars are listed in Table 7 and the emission features are shown in Figs 6 and 7. In several stars, namely 6, 18, 20, 24, 26, 28, 31, 115 and 179, it could be ascertained that some probable emission features were of nebular origin by subtracting the mean background off iteratively from the two-dimensional spectra.

The spectral peculiarities associated with relatively weaker lines such as Paschen, Ca II T (8498, 8542 and 8662 Å), O I T (7772, 7774 and 7775.4 Å) and the interstellar Na I D (5896 and 5890 Å) have also been investigated. We have determined the integrated equivalent width for Ca II T lines only for F, K and G type as these lines merge with Paschen lines of hydrogen in early-type stars. The equivalent widths of the Na I D lines are determined for all the stars. A typical uncertainty of 5–10 per cent is assigned to these determinations as is seen from repeating the width measurements. The values obtained in this way are tabulated in Table 5. The EWs of the O I T lines are too weak ($\leqslant$0.3 Å) to estimate with low-resolution spectra and in a few cases due to the low S/N ratio of the spectra. However, individual cases of enhanced O I T absorptions are noted in the following subsections along with the Paschen line peculiarities.

The Ca II T lines have been used to explore the disc frequency and disc accretion rate in late-type pre-main-sequence (PMS) candidates (see Hillenbrand et al. 1998). It can be inferred using transformations by Gullbring et al. (1998) that an EW (Ca II T) ≈ -3 Å corresponds to $\dot{M}_{\rm acc} \leqslant 10^{-8}\,{\rm M}_{\odot}\,{\rm yr}^{-1}$ and at lower resolution as in the present case $\dot{M}_{\rm acc} < 10^{-8}\,{\rm M}_{\odot}\,{\rm yr}^{-1}$ should correspond to filled-in Ca II T lines. The Ca II T widths were determined for 54 stars. The mean value, best represented by 32 non-emission MS stars, is 2.9 ± 0.3 (s.d.) Å, which is comparable to the value quoted for Ca II T widths

Table 6. Adopted spectral types, colour excesses and R_V of all programme stars. Asterisked ones are either the new or modified spectral types from the present study. Columns 11 and 12 provide equivalent widths (EW) for the Ca II triplet (~8500 Å) and Na I doublet (5890/5896 Å). The 'Grp' column provides the grouping sequence according to their reddening behaviour (see Section 4) while the finally adopted membership is given in the last column in which 'M', 'NM' and 'PM' stand for member, non-member and probable member (see Section 6).

ID	SpT	$E(U-V)$	$E(B-V)$	$E(V-R)$	$E(V-I)$	$E(V-J)$	$E(V-H)$	$E(V-K)$	R_V	EW(Å) Ca II T	EW(Å) Na I D	Grp	Memb
1	B2.5 IV	0.33	0.23	0.20	–	0.69	0.71	0.79	3.78		0.45	2	M
2	K2 IV	1.21	0.57	–	–	1.36	1.62	1.69	3.26	2.87	1.11	1	M
3	B8 V	1.62	0.80	0.53	1.07	1.83	2.11	2.29	3.15		0.35	1	M
4	G8 V	0.32	0.20	–	–	0.41	0.52	0.56	–	3.08	0.93	1	M
5	F8 Ve	0.61	0.33	0.17	0.39	1.07	1.55	2.03	4.42	−0.26	0.73	3	M
6	G9 IV–Ve	0.05	0.36	0.14	0.31	0.95	1.27	1.45	3.60	1.80	1.06	2	M
7	B8	1.47	0.82	0.58	1.15	1.90	2.18	2.29	3.07		0.20	1	M
8	A2 IIIe*	0.90	0.52	0.41	0.77	1.26	2.01	2.75	3.31		0.45	3	M
9	A1	0.82	0.44	0.26	0.49	0.85	0.91	1.02	2.55		0.18	3	M
10	G0 V	0.21	0.21	0.12	0.33	0.79	0.97	0.97	5.08	2.75	0.61	2	M
11	A0	0.86	0.58	0.42	0.68	1.31	1.54	1.70	3.22		0.29	1	M
12	F8	1.46	0.74	0.59	1.05	2.11	2.51	2.84	3.89	2.65	0.49	2	M
13	B2 V	0.53	0.33	0.28	0.65	1.26	1.45	1.68	5.60		0.43	2	M
14	B3 V	0.83	0.56	0.38	0.88	1.84	2.27	2.48	4.48		0.41	2	M
15	K0 Ve	0.73	0.55	0.30	1.00	1.94	2.25	2.42	4.84	3.54	0.64	2	M
16	A2	0.39	0.28	–	–	0.71	0.85	0.96	3.77		0.40	2	M
17	B0 V	1.42	0.53	–	–	2.77	3.19	3.22	6.68		0.25	2	M
18	B0.5 V	0.43	0.31	0.34	0.70	2.58	2.88	2.80	9.94		0.38	3	M
19	A0	0.14	0.22	–	–	1.06	1.27	1.44	7.20		0.19	2	M
20	A1 V	0.46	0.32	0.27	0.65	1.27	1.51	1.65	5.67		0.63	2	M
21	B0.5 V	0.55	0.36	0.30	0.66	1.26	1.54	1.74	5.32		0.27	2	M
22	O7 e	0.52	0.30	0.28	0.66	1.35	1.69	1.89	6.14		0.30	2	M
23	G0 IV–IIIe	0.94	0.47	0.27	0.65	1.35	1.70	1.84	2.92	1.95	0.87	2	M
24	B2 V	0.94	0.56	0.23	0.83	2.08	2.64	2.93	5.07		0.33	2	M
25	O9.5 V	0.36	0.22	0.16	–	0.84	0.96	1.11	5.55		0.34	2	M
26	G8 V	0.20	0.16	0.16	0.57	1.02	1.31	1.34	–	2.74	1.26	2	M
27	G3 IV–Ve	1.91	1.21	0.43	1.24	2.07	2.86	3.71	2.33	−1.54	0.44	3	M
28	G3 IV–V	0.34	0.31	0.25	0.46	0.84	1.07	1.19	4.22	2.61	0.64	2	M
29	G8 Ve	1.39	0.41	0.13	0.61	1.06	1.39	1.48	3.53	2.32	0.88	2	M
30	B0.5 V	0.85	0.54	0.40	0.85	1.72	1.99	2.15	4.38		0.60	2	M
31	G9 IV–Ve	0.71	0.37	0.12	0.65	1.12	1.47	1.62	4.13	2.56	1.22	2	M
32	K2 IVe	0.33	0.25	–	0.41	1.16	1.41	1.76	6.33	1.64	0.95	3	M
33	K2 Ve	0.48	0.28	0.12	0.72	1.01	1.22	1.51	4.92	1.33	1.13	3	M
34	K1 Ve	0.71	0.33	0.22	0.49	1.21	1.45	1.53	5.10	1.90	1.05	2	M
35	A3 IIIe*	0.66	0.33	0.03	0.30	1.58	2.57	3.65	6.53		0.42	3	M
36	B4 V	1.28	0.81	0.67	1.40	2.84	3.44	3.77	4.48		0.41	2	M
37	A0	0.15	0.20	0.17	0.36	0.71	0.75	0.88	4.84		0.17	2	M
38	F6 IV	0.46	0.26	0.12	0.40	0.80	0.93	0.99	4.19	3.12	0.30	2	M
39	G6*	0.41	0.11	0.10	0.40	0.33	0.40	0.42	–	2.70	0.68	3	M
40	A7	0.03	0.06	–	–	0.25	0.24	0.29	–		0.22	2	M
41	B5 V	1.41	0.87	0.73	1.39	2.40	2.74	2.91	3.68		0.11	2	M
42	F6	2.13	1.12	0.47	–	2.65	3.16	3.36	3.30	3.03	0.50	1	M
43	A6*	0.32	0.20	0.16	0.26	0.66	0.75	0.78	4.29		0.29	2	M
44	A0*	0.92	0.70	0.42	0.90	1.53	1.75	1.82	2.86		0.23	3	M
45	G0 III	0.70	0.41	–	–	1.10	1.29	1.39	3.73	2.50	0.50	2	M
46	F9 V	0.19	0.19	–	–	0.47	0.52	0.53	–	2.20	0.41	1	M
47	G6*	1.29	0.53	–	–	1.71	2.06	2.23	4.63	2.76	0.75	3	NM
48	F6 V	−0.04	−0.02	–	–	0.24	0.30	0.28	–	1.65	0.37	3	NM
49	A1 IV	0.48	0.21	–	–	0.52	0.50	0.61	3.20		0.37	1	M
50	B9 V	0.98	0.58	–	–	1.40	1.51	1.65	3.13		0.37	1	M
51	F1 V	0.31	0.14	–	–	0.43	0.40	0.43	–	2.35	0.44	3	NM
52	B2.5 II-III	1.62	0.91	–	1.38	2.45	2.80	3.03	3.66		0.59	2	M
53	K5	1.20	0.51	–	0.63	1.23	1.45	1.61	3.47	3.23	0.96	3	NM
54	F4*	0.12	0.05	–	0.19	0.35	0.42	0.47	–	2.47	0.38	3	NM
55	A7 V	0.28	0.13	–	–	0.36	0.35	0.37	–		0.42	3	NM
56	B2 V	0.66	0.40	0.31	0.58	0.97	1.11	1.16	3.19		0.46	1	M
57	B0.5 V	0.78	0.42	0.40	0.74	1.13	1.30	1.40	3.67		0.48	3	M
58	O8 V	0.87	0.46	0.31	0.67	1.10	1.27	1.34	3.20		0.57	1	M
59	F4 V	0.12	0.07	–	–	−0.07	−0.07	−0.06	–	2.32	0.42	3	NM
60	F7	0.73	0.34	–	–	1.19	1.38	1.45	4.69	2.06	0.49	2	PM

Table 6 – *continued*

ID	SpT	$E(U-V)$	$E(B-V)$	$E(V-R)$	$E(V-I)$	$E(V-J)$	$E(V-H)$	$E(V-K)$	R_V	EW(Å) Ca II T	EW(Å) Na I D	Grp	Memb
61	B8 V	0.53	0.33	–	0.42	0.81	0.90	0.92	3.07		0.37	2	M
62	A5	0.53	0.34	–	0.52	0.96	1.03	1.15	3.72		0.54	2	M
63	G7 III	0.24	0.15	–	0.23	0.41	0.44	0.53	–	3.00	0.67	3	NM
64	O8.5 V	1.02	0.49	0.42	0.75	1.19	1.33	1.39	3.12		0.48	1	M
65	B0 V	0.71	0.38	0.34	0.63	1.10	1.24	1.27	3.68		0.46	2	M
66	B8 V	0.67	0.43	–	0.58	1.09	1.23	1.34	3.43		0.32	2	M
67	O5 V	0.81	0.48	0.27	0.58	1.01	1.15	1.25	2.86		0.50	1	M
68	B4 V	0.74	0.45	0.53	1.34	1.15	1.32	1.47	3.59		0.46	2	M
69	A2 V	0.07	0.03	0.17	0.17	0.15	0.10	0.17	–		0.24	3	NM
70	B1 V	0.67	0.40	0.26	0.55	1.01	1.12	1.21	3.33		0.58	2	M
71	B2.5 V	0.77	0.48	–	0.60	1.15	1.29	1.41	3.23		0.50	2	M
72	B9 V	0.73	0.47	0.88	1.54	1.18	1.33	1.49	3.49		0.35	2	M
73	B3 V	0.48	0.39	0.23	0.48	0.98	1.15	1.20	3.38		0.57	2	M
74	B2.5 V	0.77	0.49	0.36	0.70	1.22	1.36	1.48	3.32		0.44	2	M
75	O9 V	0.91	0.45	0.31	0.66	1.13	1.27	1.39	3.40		0.45	1	M
76	B2 V	0.85	0.48	0.29	0.60	1.14	1.30	1.39	3.19		0.47	1	M
77	B7 V	0.87	0.58	–	0.61	1.40	1.60	1.79	3.39		0.45	2	M
78	B6 V	0.66	0.45	0.37	0.70	1.17	1.37	1.45	3.54		0.42	2	M
79	B8 IV	0.68	0.43	–	0.57	1.14	1.36	1.46	3.73		0.37	2	M
80	B0.5 V	0.72	0.42	0.24	0.55	1.03	1.16	1.22	3.20		0.34	1	M
81	O4 V	0.93	0.53	0.30	0.69	1.22	1.42	1.51	3.13		0.37	1	M
82	B3 V	0.89	0.50	0.28	0.65	1.37	1.67	2.04	3.74		0.43	3	M
83	B6 V	0.86	0.55	–	0.74	1.37	1.54	1.64	3.28		0.52	2	M
84	O9.5 V	1.47	0.84	0.49	1.11	2.18	2.51	2.67	3.50		0.43	2	M
85	F3 V	0.59	0.21	–	–	0.53	0.54	0.61	3.20	3.10	0.47	3	NM
86	G1 V	0.32	0.17	–	–	0.48	0.57	0.62	–	2.80	0.43	3	NM
87	K3 Ibe	1.62	0.77	–	–	1.91	2.66	2.63	3.38	4.56	1.44	3	PM
88	F9 V*	0.25	0.06	0.03	0.10	0.32	0.36	0.41	–	2.55	0.34	3	M
89	F9*	0.28	0.18	0.17	0.30	0.65	0.82	0.87	–	2.37	0.36	3	M
90	K1 V	3.93	1.66	0.73	1.91	3.26	3.87	4.20	2.68	3.58	0.96	3	NM
91	G0 e*	0.02	0.03	0.13	0.07	0.27	0.32	0.36	–	3.04	0.20	3	PM
92	F8 Ve*	0.52	0.25	0.13	0.35	0.68	0.91	1.12	3.71	1.95	0.62	3	M
93	G5*	1.89	0.91	0.57	–	2.30	2.69	2.89	3.49	3.01	0.76	3	NM
94	B3	1.71	0.91	0.67	1.62	3.15	3.88	4.36	4.71		0.24	3	PM
95	B2 V	1.24	0.86	0.55	1.43	2.96	3.62	4.04	4.77		0.59	3	PM
96	G0 IV–V	0.04	0.02	−0.04	0.11	0.27	0.34	0.37	–	3.14	0.61	3	M
97	B8 IIIe*	0.69	0.25	0.39	0.93	1.53	2.55	3.75	8.35		0.49	3	M
98	A2 IVe	0.11	0.08	0.07	0.21	0.43	0.79	1.47	–		0.44	3	M
99	F8 Ve	0.50	0.33	0.11	0.31	0.86	1.10	1.17	3.90	1.93	0.71	3	M
100	G5 Ve	0.47	0.26	−0.01	0.17	0.51	0.79	1.11	2.70	0.06	0.73	3	M
101	G8 Ve	0.29	0.21	0.10	0.21	0.56	0.87	1.28	3.64	2.38	0.45	3	M
102	F9*	0.23	0.10	−0.05	0.00	0.21	0.31	0.32	–	2.82	0.34	3	M
103	K0*	2.28	1.14	0.70	1.48	2.75	3.17	3.45	3.33	3.13	0.69	3	NM
104	A2*	0.99	0.56	0.15	–	1.27	1.44	1.56	3.06		0.53	1	NM
105	K0*	1.67	0.86	0.26	–	1.83	2.18	2.34	2.99	2.83	0.67	3	NM
106	G8	1.08	0.27	−0.02	0.07	0.37	0.51	0.56	2.28	3.15	0.89	3	NM
107	O7	0.54	0.29	–	–	0.71	0.84	0.92	3.49		0.56	2	M
108	B0.5	0.52	0.29	0.16	0.37	0.77	0.79	0.88	3.34		0.52	2	M
109	B5 e	0.37	0.29	–	–	0.82	1.04	1.27	3.86		0.68	3	M
110	O4 V	0.64	0.35	0.27	0.53	0.94	1.10	1.18	3.71		0.58	2	M
111	B0 V	0.49	0.30	–	0.38	0.74	0.82	0.86	3.15		0.52	2	M
112	B4	0.61	0.35	–	0.48	0.97	1.13	1.18	3.71		0.58	2	M
113	B8	0.24	0.36	–	0.59	1.15	1.45	1.60	4.89		0.29	2	M
114	F4 I*	0.49	0.24	0.33	0.73	0.81	0.90	0.96	4.40	5.07	0.42	3	NM
115	B2 e	1.98	1.05	0.63	1.46	3.12	3.99	4.44	4.05		0.67	3	M
116	B3 V	0.40	0.31	0.28	0.53	0.94	1.10	1.20	4.26		0.58	2	M
117	G7	0.92	0.41	–	0.50	1.00	1.17	1.29	3.46		0.86	3	NM
118	B2 V	0.34	0.28	0.18	0.37	0.72	0.80	0.89	3.50		0.56	2	M
119	B2	0.41	0.33	–	0.18	0.77	0.72	0.83	3.17		0.63	2	M
120	B8	0.44	0.30	–	0.58	1.16	1.42	1.58	5.79		0.39	2	M
121	B1.5 V	0.52	0.35	0.16	0.44	0.95	1.08	1.20	3.77		0.62	2	M
122	B2 V	0.58	0.42	0.24	0.62	1.31	1.63	1.99	4.25		0.68	3	M
123	B2 V	0.49	0.33	0.15	0.42	1.05	1.19	1.34	4.47		0.67	2	M

Table 6 – *continued*

ID	SpT	$E(U-V)$	$E(B-V)$	$E(V-R)$	$E(V-I)$	$E(V-J)$	$E(V-H)$	$E(V-K)$	R_V	EW(Å) Ca II T	EW(Å) Na I D	Grp	Memb
124	B1 V	0.62	0.33	0.18	0.46	0.96	1.13	1.22	4.07		0.60	2	M
125	B2 V	0.56	0.36	–	0.47	0.96	1.09	1.15	3.51		0.75	2	M
126	B0 IVe	0.78	0.46	0.32	0.76	1.45	1.74	2.13	4.30		0.38	3	M
127	B2 V	0.51	0.35	0.16	0.44	0.89	1.04	1.12	3.52		0.91	2	M
128	B2 V	0.59	0.39	0.14	0.41	1.02	1.17	1.29	3.64		0.85	2	M
129	B2 IV	0.53	0.32	–	–	0.85	0.90	1.02	3.51		0.50	2	M
130	B2.5 V	0.48	0.32	–	0.48	0.93	1.11	1.20	4.13		0.72	2	M
131	B2.5 V	0.22	0.28	0.21	0.39	0.81	0.90	1.01	3.97		0.62	2	M
132	B1 V	0.50	0.33	–	0.49	0.97	1.10	1.18	3.93		0.68	2	M
133	B2.5 V	0.46	0.35	0.22	0.45	0.94	1.24	1.26	3.66		0.58	2	M
134	B0.5 V	0.62	0.41	–	–	1.02	1.14	1.22	3.27		0.86	2	M
135	B2 V	0.63	0.40	0.06	0.35	0.87	1.05	1.22	3.36		0.65	2	M
136	B2 IV	0.38	0.26	0.23	0.44	0.67	0.95	1.09	4.51		0.56	3	M
137	B2 V	0.62	0.33	–	0.51	0.98	1.10	1.22	4.07		0.50	2	M
138	B2 V	–	0.33	–	–	0.73	0.85	0.93	3.10		0.48	1	M
139	B6	0.32	0.31	–	0.46	0.81	0.88	0.95	3.37		0.40	2	M
140	B3	0.55	0.36	0.26	0.50	1.05	1.18	1.27	3.88		0.55	2	M
141	B2.5 V	0.74	0.47	0.30	0.64	1.30	1.57	1.70	3.98		0.85	2	M
142	O6.5 V	0.74	0.41	0.25	0.55	1.11	1.28	1.34	3.60		0.67	2	M
143	K5	0.13	0.13	–	0.00	0.05	0.00	0.01	–	3.38	1.15	3	NM
144	B6	0.61	0.38	–	0.62	1.27	1.50	1.65	4.78		0.70	2	M
145	K2	0.44	0.32	–	0.34	0.35	0.34	0.41	1.41		0.75	3	NM
146	B2	0.67	0.40	0.25	0.50	1.31	1.51	1.66	4.57		0.65	2	M
147	B3	0.76	0.48	–	–	1.20	1.45	1.58	3.62		0.82	2	M
148	B8	0.64	0.52	–	–	1.45	1.70	1.84	3.89		0.60	2	M
149	K7 I-III*	2.28	1.17	–	–	2.64	3.33	3.67	3.68	6.41	2.63	3	PM
150	B6	1.63	1.00	0.74	1.41	2.60	2.94	3.16	3.48		0.22	2	M
151	K7 III–IV*	2.68	1.30	–	–	2.75	3.42	3.63	3.26		2.20	3	PM
152	B1 V	1.12	0.73	0.44	0.99	1.85	2.08	2.23	3.36		1.17	2	M
153	B0.5 V	1.25	0.75	0.48	1.04	1.93	2.22	2.33	3.42		0.76	2	M
154	O8.5 V	2.29	1.33	0.88	1.97	3.76	4.34	4.70	3.89		0.45	2	M
155	05.5 V	1.92	1.12	0.74	1.68	3.15	3.68	3.97	3.90		0.60	2	M
156	O6.5 V	1.26	0.76	0.49	1.08	1.96	2.22	2.43	3.52		0.68	2	M
157	O4 V	1.27	0.77	0.53	1.18	2.04	2.40	2.59	3.70		0.60	2	M
158	B1 V	1.43	0.91	0.56	1.28	2.27	2.60	2.78	3.36		0.51	2	M
159	B1.5 V	1.61	0.94	0.52	1.17	2.38	2.80	3.00	3.51		0.53	2	M
160	B2	1.41	1.07	0.72	1.61	2.98	3.51	3.99	3.80		0.42	3	M
161	O7 IIb	2.01	1.19	0.77	1.65	3.05	3.57	3.80	3.51		0.68	2	M
162	B1 V	1.18	0.70	0.40	0.95	1.86	2.15	2.30	3.61		0.40	2	M
163	B0.5 V	1.69	1.01	0.66	1.45	2.64	3.05	3.23	3.52		0.63	2	M
164	O9.5 V	1.23	0.79	0.42	1.01	1.78	2.00	2.18	3.04		0.99	1	M
165	B2 V	1.33	0.77	0.67	1.28	2.18	2.50	2.66	3.80		1.04	2	M
166	B1.5 V	1.53	0.88	0.58	1.30	2.42	2.79	2.90	3.63		0.66	2	M
167	B0 V	1.46	0.92	0.57	1.26	2.35	2.64	2.85	3.41		0.75	2	M
168	B1 V	1.83	1.08	0.81	1.66	2.97	3.43	3.72	3.79		0.98	2	M
169	O9.5 V	0.88	0.58	0.32	0.71	1.33	1.48	1.56	2.96		0.71	1	M
170	O8.5 V	1.11	0.71	0.46	1.00	1.84	2.14	2.30	3.56		0.85	2	M
171	O9.5 I	0.95	0.61	0.38	0.85	1.37	1.52	1.65	2.98		0.90	1	M
172	B1 V	0.79	0.55	0.28	0.68	1.35	1.51	1.60	3.20		0.78	2	M
173	B0.5 Ve	1.09	0.70	0.42	0.94	1.77	2.01	2.21	3.47		0.67	2	M
174	B5 e	0.94	0.59	0.36	0.78	1.44	1.61	1.80	3.36		0.81	2	PM
175	B1 e	0.91	0.58	1.07	1.71	2.24	2.64	3.03	5.27		0.61	3	M
176	B2.5 I	2.27	1.30	0.82	1.79	3.46	3.96	4.30	3.64		0.83	2	PM
177	G9*	1.36	0.55	–	–	1.40	1.62	1.76	3.52		0.84	3	NM
178	G6	1.44	0.56	0.33	0.68	1.37	1.65	1.83	3.59		1.22	3	NM
179	B1.5 V	0.99	0.62	0.38	0.86	1.52	1.80	1.98	3.51		0.92	2	M
180	B1	–	0.64	–	–	1.77	1.92	2.11	3.63		0.67	2	M
181	B9 V	–	0.41	–	–	1.06	1.16	1.25	3.35		0.54	3	NM
182	A0 III	–	0.41	–	–	1.19	1.29	1.45	3.89		0.49	3	NM
183	B9.5 IV	–	0.21	–	–	0.70	0.75	0.84	4.40		0.57	3	NM
184	B9 IV	–	0.18	–	–	0.90	1.03	1.15	–		0.57	3	NM
185	K0*	–	0.43	–	–	0.97	1.12	1.23	3.15		0.74	3	NM
186	A0 IV	–	0.19	–	–	0.78	0.88	0.97	–		0.63	3	M

Table 6 – *continued*

ID	SpT	$E(U-V)$	$E(B-V)$	$E(V-R)$	$E(V-I)$	$E(V-J)$	$E(V-H)$	$E(V-K)$	R_V	EW(Å) Ca II T	EW(Å) Na I D	Grp	Memb
187	B1.5	–	0.59	–	–	1.56	1.79	1.87	3.49		0.67	3	NM
188	B0.5 IV	1.87	1.10	–	–	2.34	2.63	2.79	2.79		0.70	1	M
189	B2 V	1.52	0.96	–	–	2.23	2.50	2.63	3.01		0.85	1	M
190	O8 V	1.78	1.09	–	–	2.43	2.76	2.88	2.91		1.00	1	M
191	B2 V	1.60	0.99	–	–	2.20	2.47	2.64	2.93		0.87	1	M
192	B1.5 V	1.41	0.95	–	–	1.95	2.24	2.36	2.73		0.87	1	M
193	B1.5 V	1.64	0.95	–	–	1.96	2.26	2.42	2.80		0.97	1	M
194	G8 III	1.46	0.76	–	–	1.46	1.49	1.74	2.62	3.39	0.98	3	NM
195	B0.5 I	1.93	1.08	0.68	1.25	2.32	2.60	2.71	2.76		0.83	3	PM
196	B4 V	1.13	0.77	–	–	1.94	2.25	2.40	3.43		0.45	1	M
197	B0 IV	1.22	0.74	–	–	1.69	1.88	2.00	2.97		0.90	1	M
198	B1 III	1.86	1.07	–	–	2.14	2.26	2.51	2.73		0.82	3	M
199	K8 V	1.38	0.62	–	–	1.16	1.34	1.52	2.70	2.98	1.20	3	NM
200	B2.5 V	1.30	0.88	–	–	1.87	2.15	2.35	2.94		0.74	1	M
201	B1.5 V	1.11	0.82	–	–	1.94	2.14	2.31	3.10		0.91	1	M
202	O7 V	1.46	0.88	0.54	1.16	2.08	2.38	2.49	3.11		0.39	1	M
203	B0.5 V	1.72	1.04	0.63	1.33	2.44	2.74	2.90	3.07		0.47	1	M
204	B0.5 V	1.63	1.02	0.62	1.32	2.31	2.75	2.95	3.18		0.81	1	M
205	B1 V	1.61	0.99	–	–	2.43	2.74	2.92	3.24		0.42	1	M
206	F8 V	0.25	0.22	–	–	0.63	0.71	0.75	3.75	2.84	0.87	3	NM
207	B1 V	1.75	1.06	–	–	2.65	2.99	3.19	3.31		0.53	1	M
208	F2 IV	0.05	0.11	–	–	0.31	0.32	0.34	–	2.75	0.69	3	NM
209	A9	1.83	1.08	0.64	1.21	2.10	2.57	2.71	2.65		0.45	3	NM
210	B0.5 V	1.93	1.15	–	–	2.69	3.04	3.23	3.09		0.46	1	M
211	F8 Ib	1.29	0.66	–	–	1.40	1.60	1.72	2.87	4.43	0.54	3	NM

(∼3 Å) for late-type MS stars by Hillenbrand et al. (1998). There are stars having larger than 3σ discrepancy (see Fig. 8a). The stars 87, 114, 149 and 211 have widths greater than 3.9 Å; two of these are classified as supergiants in the literature, therefore we assign the supergiant (I) luminosity to the other two stars (114, 149). There are 11 stars with widths less than 2 Å indicating the presence of a circumstellar disc; moreover all of these except star 48 also show weak to strong emission features. For stars 5, 27 and 100, the width is near zero or negative indicating the presence of an accretion disc ($\sim 10^{-8}$ $M_\odot$ yr^{-1}), while stars 6, 23, 32, 33, 34, 48, 92 and 99 have values between 1 and 2 Å, qualifying them for having circumstellar discs with low accretion rate $\leqslant 10^{-8}$ $M_\odot$ yr^{-1}.

The dependence of Na I D linewidths on spectral types indicates higher values for late-type stars (F, G, K) as the measure is affected by the stellar components (Fig. 8b). A large scatter (0.3–1.0 Å) for B-type stars is measured, which indicates surplus circumstellar and intracluster gas components in addition to the normal extinction effects. The largest scatter in Na I D width is seen for the clusters NGC 1976 and NGC 2264. The average values and standard deviation of the Na I D width determined from early-type PM members for clusters NGC 1976, NGC 2264, NGC 2244, NGC 6530, NGC 6823 and NGC 6611 are 0.18 ± 0.04, 0.22 ± 0.02, 0.45 ± 0.07, 0.60 ± 0.15, 0.71 ± 0.20 and 0.70 ± 0.18 Å, respectively. These values appear to show a weak correlation with the corresponding galactocentric distances to the clusters (see Fig. 8c); however, it is difficult to discuss the extinction effects on the Na I D widths due to circumstellar and intracluster dust and gas.

Though most of the peculiarities are listed in Table 7 and also included in notes to Table 4, we describe spectral features for specific interesting stars in their spectral-type sequences.

There are 22 O-type stars in our sample. Eleven of these stars (107, 142, 154, 155, 156, 157, 161, 164, 169, 170, 171) have been observed only in the blue. The spectral features characteristic of Of stars are seen clearly in our spectra (see Fig. 4). For example, the stars 81, 110, 67, 155 and 156 show N III 4630–4634 Å line in emission. Moreover, He II 4686 Å is also seen in emission for star 161 (a bright giant, IIb) confirming the reported spectral features from dispersions much higher than ours. In a sample of 109 B-type stars (86 early-type – up to B4), 29 stars are reported to have weak to strong emission features. Seventeen of these are reported by Hiltner, Morgan & Neff (1965) on MK region observations for NGC 6530 with a caution for effects of nebulosity. We have Hα region spectra for only four stars, namely 78, 97, 188 and 205. Altogether we could confirm Balmer emissions only in seven of them, viz. 97, 122, 126, 160, 173, 174 and 175. A strong O I T absorption in star 97 (EW ∼ 0.83 Å) indicates that it is not a dwarf. The width of O I T features comes out to be around 0.3 Å for dwarfs. Star 97 is the only one which shows Paschen lines in weak emission. About 8 per cent of our sample shows characteristics of Be stars which is well in accordance with the general percentage of Be stars, i.e. 11 per cent (Jaschek & Jaschek 1987). The luminosity effects can be seen as sharper balmer lines for the stars 176 (B2.5 I), 195 (B0.5 Ib), 52 (B2.5 II–III) and 198 (B1 III); however, it is less evident for stars 1, 79, 183, 184 and 188 reported as subgiants in the literature.

A total of 20 A-type stars was observed. Our spectra show Hα in strong single-peak emission for star 35. A strong O I T in absorption in the star 35 (EW ∼ 0.85 Å) according to the relation obtained by Danks & Dennefeld (1994) indicates that this is a candidate Herbig Ae/Be (HAB) star. The spectrum of star 8 shows sharp Balmer lines with enhanced Ca II T absorption, very weak Hα absorption and large Na I D absorption, indicating a PMS star with weak core emission at Hα having a circumstellar shell and making it another candidate HAB star. The stars 149 and 151 are of special interest as they are reported to have post-AGB characteristics. The TiO bands around

Table 7. List of stars with emission features and spectral peculiarities. Asterisked stars are reported in the present work for the first time along with some additional features reported for stars 5, 100 and 101. Stars with a plus symbol are optical variables and stars 5, 6, 27 and 29 are NIR variables (Carpenter 2001).

ID	SpT	Emission peculiarities
5+	F8 V	Ca II HK in core emission, strong Hα, filled Hβ
6*	G9 IV–V	Ca II HK in emission
8*	A2 III	Hα partially filled in emission
15*+	K0 V	Ca II HK in emission on wide absorption
22	O7	Hα partially filled in emission
23*	G0 III–IV	Ca II HK partially filled, Hα in weak emission
27+	G3 IV–V	Ca II HK and Balmer lines in emission
29*	G8 V	Ca II HK partially filled, Hα in weak emission
31	G9 IV–V	Ca II HK in emission on absorption
32+	K2 IV	Ca II HK in emission, Hα in strong emission
33+	K2 V	Ca II HK and Balmer lines in emission
34	K1 V	Ca II HK in filled emission, weak Hα emission
35+	A3 III	Hα in strong emission
87*	K3 Ib	Ca II HK in emission
91*	G0	Ca II HK weak emission on wide absorption
92*	F8 V	Hα partially filled in emission
97+	B8	Hα in strong emission, Hβ partially filled
98+	A2 IV	Hα totally filled in emission
99*	F8 V	Ca II HK partially filled, Hα totally filled
100+	G5 V	Ca II HK in emission, Hα in strong emission
101+	G8 V	Ca II partially filled, Hα in strong emission
109*	B5	Hβ in emission, Hγ partially filled in emission
115*	B2	Hβ and Hγ partially filled in emission
122	B2 V	Hβ in emission, Hγ partially filled in emission
126	B0 IV	Hβ in emission, Hγ partially filled in emission
160	B2	Hβ in emission
173	B0.5 V	Hβ partially filled in emission
174	B5	Hβ totally filled in emission
175	B1	Hβ totally filled in emission

6651 Å and 7054 Å can be seen very clearly in both of these stars along with a weak appearance in star 199. The MK spectra of star 149 matches best with K7 III (BD+590128 – a MK standard from the Jacoby library). The Ca II T width for this star indicates that it is a supergiant. Therefore, we classify these stars (149, 151) as giants of type K7; however, the star 149 may be a candidate supergiant.

Table 8 summarizes the distribution of all the programme stars according to their spectral type, luminosity class and emission-line peculiarities.

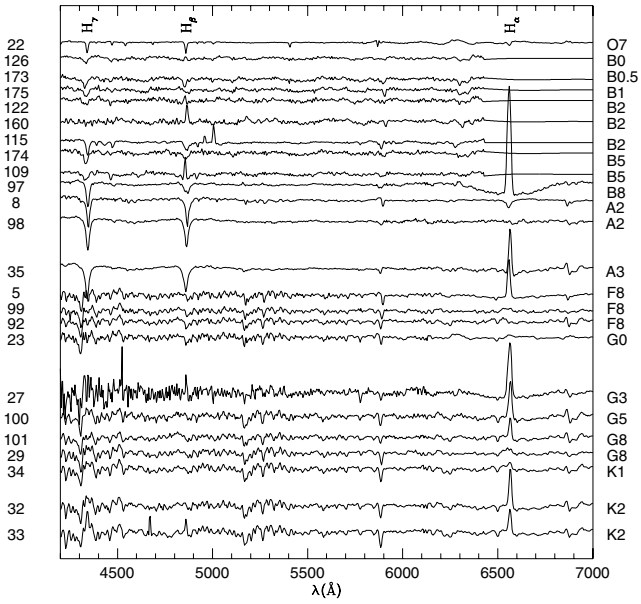

Figure 6. Spectra in the wavelength range 4200–7000 Å of stars having emission features in Balmer lines.

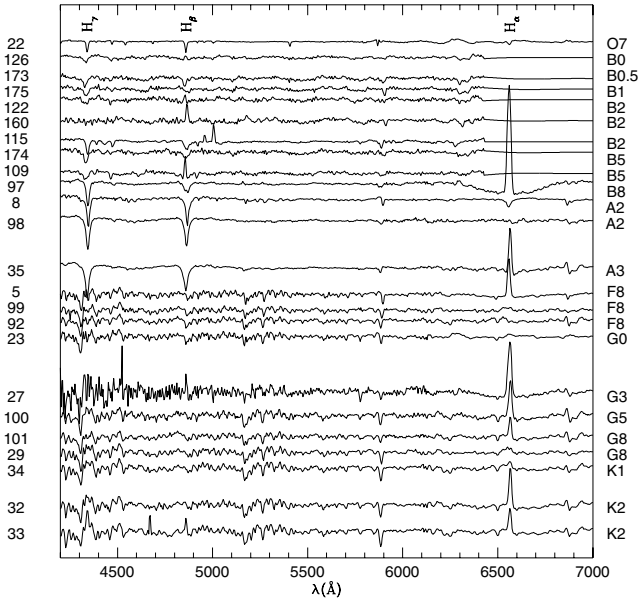

Figure 7. Spectra in the wavelength range 3800–4800 Å of stars having emission features in Ca II H, K lines. The stars 27 and 33 have emission spectra.

4 EXTINCTION PROPERTIES

4.1 Intrinsic colours and colour excesses

To study the behaviour of reddening and extinction properties, we derive $E(U-V)$, $E(B-V)$, $E(V-R)$, $E(V-I)$, $E(V-J)$, $E(V-H)$ and $E(V-K)$ colour excesses of the cluster members using the MKK spectral-type–luminosity-class–colour relation given by FitzGerald (1970) for $(U-V)$ and $(B-V)$; by Johnson (1966) for $(V-R)$ and $(V-I)$, transformed to the Cousins system using Bessell's transformation (1979); and by Koornneef (1983) for $(V-J)$, $(V-H)$, and $(V-K)$. Maximum uncertainties in the colour excess determination in *UBVRI* is considered to be about ∼0.08 mag and in *JHK* to be ∼0.15 mag. The quoted uncertainties include the effect on the derived intrinsic colours from a sample of field stars with various degrees of evolution within the MS. The colour excesses in some bands are found to be negative for stars 48, 59, 96, 100, 102 and 106 but the values are within the uncertainty limit. Most probably, this is due to non-simultaneous observations and/or due to variability of the star.

We have determined the value of R_V using A_V which is approximated as 1.1 $E(V-K)$. The ratio of A_V to $E(V-K)$ does not change appreciably with R_V value (Whittet & van Breda 1980). He et al. (1995) estimated the A_V by different methods and concluded that they agree to better than 3 per cent for normal stars. However, the value of R_V is very sensitive to the excess radiation in the K band as well as to very small values of $E(B-V)$. Therefore the value of

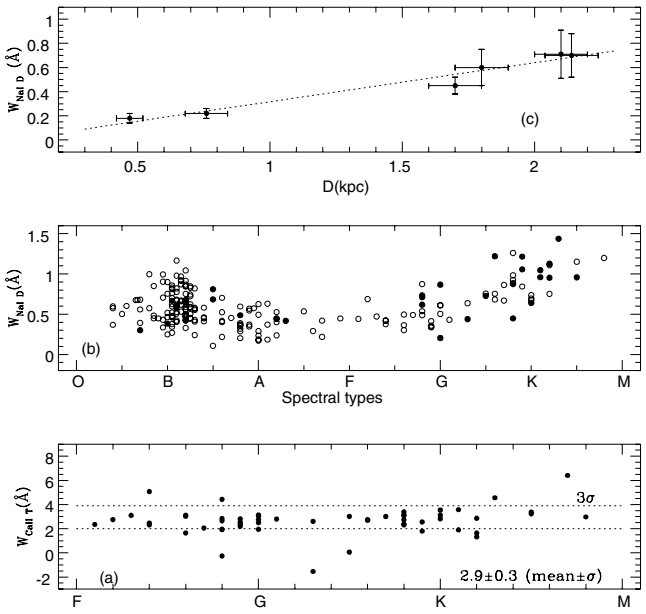

Figure 8. Equivalent widths of Ca II triplet lines (8498, 8542 and 8662 Å) and of Na I doublet lines (5890 and 5896 Å) are plotted against spectral types in panel (a) and (b), respectively. The average values of the Ca II triplet width for non-emission stars are written in panel (a) and the dotted lines are drawn to show 3σ limits. Filled circles in panel (b) are emission-line stars. Panel (c) shows the median Na I D widths against cluster distances for NGC 1976, 2244, 2264, 6530, 6611 and 6823.

Table 8. Distributions of spectral types and luminosity classes among the programme stars. The luminosity class of emission objects is discussed in the text.

SpT	N	Luninosity types					Emission line stars
		I	II	III	IV	V	(H I, Ca II HK, both)
O	22	1	1			19	1 (1, –, –)
B	109	2		2	5	91	9 (9, –, –)
A	20			1	2	14	3 (3, –, –)
F	20	2			2	13	3 (3, 2, 2)
G	24			3		13	8 (5, 8, 5)
K	16			1	1	9	5 (3, 5, 3)
Total	211	5	1	7	10	159	29

A_V for a sample of 41 stars, found to have anomalous radiation in the NIR (see Section 5), are determined using $E(V-J)$ assuming normal reddening. Table 6 contains values of R_V estimated in this way for all the programme stars except for those 23 stars which have very low values (<0.2 mag) of $E(B-V)$.

In order to understand the properties of interstellar matter in the direction of clusters, we plot the ratios of colour excesses $E(U-V)$, $E(B-V)$, $E(V-R)$, $R(V-I)$, $E(V-H)$ and $E(V-K)$ against $E(V-J)$ in Fig. 9. These will be referred as colour excess diagrams (CEDs) hereafter. As our sample belongs to the star-forming regions and is likely to have young stellar objects, the colour excess ratios are plotted relative to $E(V-J)$ primarily with the aim of minimizing contributions from the blueing effect and ultraviolet excess on the V band as well as to minimize contributions from circumstellar dust and gas shells in the J band. Moreover, $E(V-J)$ does not depend on properties such as the chemical composition, shape, structure and degree of alignment of the interstellar matter (Qian & Sagar 1994; Yadav & Sagar 2002). In Fig. 9, the dotted lines are drawn to represent the normal interstellar extinction law (Mathis 1990). Errors expected from the observational uncertainties are shown with crosses. Most of the sample stars lie on the normal reddening line for all the clusters in the NIR CEDs, while a scatter of varying amount can be seen in diagrams with $E(U-V)$ and $E(B-V)$. It is a maximum for NGC 1976 and NGC 6611 and a minimum for NGC 2244 and NGC 6530.

We divided the stars into three groups depending upon their deviation in the CEDs with respect to the normal line. Group 1 contains all the stars following the normal law within observational uncertainty, while Group 2 stars follow the normal law in NIR and deviate towards a lower ratio in the near-ultraviolet (NUV). The effect of binarity on the observed deviations or anomalies was checked by adding together various later-type secondaries to O- and B-type stars. The binarity contribution is larger for B spectral types and is not significant in either case, compared with the quoted uncertainties. Moreover the effects are likely to be a little larger for the PMS stars as they are brighter than the MS stars for their temperature. The sample also contains peculiar stars in the sense that they do not follow a particular trend and deviate in either one or two bands in the NIR and NUV. These usually show emission features, chemical peculiarities and variability at visible or NIR wavelengths. All of these stars, along with those with very low membership, were kept in Group 3 and were not considered in estimating mean reddening for the cluster. The thirteenth column of Table 6 indicates the categorization of Group 1, 2 and 3 stars, while a number distribution for Group 1 and 2 stars is given in Table 9. A cluster-wise description of the reddening properties is given below.

4.2 Extinction law towards clusters

For NGC 1976, wide variations in the reddening values, e.g. $R_V = 4.8$ (Mendez 1967), 5.0 (Johnson 1968), and 3.1 (Walker 1969) have been reported. It has been argued that part of the large value of R_V may also be contributed by the far-infrared brightness of stars (Johnson 1967). A recent study by Qian & Sagar (1994) concludes that the cluster presents both normal as well as anomalous behaviour. The UV extinction study also suggests an anomalous galactic curve towards higher values of R_V (Bohlin & Savage 1981). Among most of our sample having high values of $E(B-V)$, there exist six stars in Group 1 which follow a normal extinction law and have a mean value of $R_V = 3.18 \pm 02$ with a range from 3.07 to 3.30 (Tables 6 and 9). Four of these [P1049(2), P1212(3), P1539(7), P1712(11)] have also been reported by Qian & Sagar (1994). The star P1360, lightly reddened (∼0.2) and located at the front edge of the cluster, is likely to exhibit normal reddening as the UV flux distribution of seven lightly reddened cluster members in NGC 1976 suggests average Galactic extinction (Panek 1983). Other stars may be affected by unresolved binaries, star-formation processes, location and evolution of the grain environment, and/or the uncertainties in the reddening determination. Group 2 stars, 28 in total, have a mean value of R_V of 4.78 ± 0.10 with a range from 3.77 to 9.94. The far-UV extinction in NGC 1976 is also significantly smaller and corresponds to a galactic average of 6.5 (Bohlin & Savage 1981; Panek 1983). A group of five stars [P1863(17), P1865(18), P1885(20), P1889(21), P1993(25)] common with the current study gives an $E(B-V)$ weighted average of $R_V = 6.74$, which is in good agreement with the value quoted by Bohlin & Savage (1981). The extinction properties do indicate a shift in the grain size distribution towards larger than normal sized particles in these regions.

The cluster NGC 2244 has a mean reddening of $E(B-V) = 0.47$ mag with a normal reddening law and a small amount of

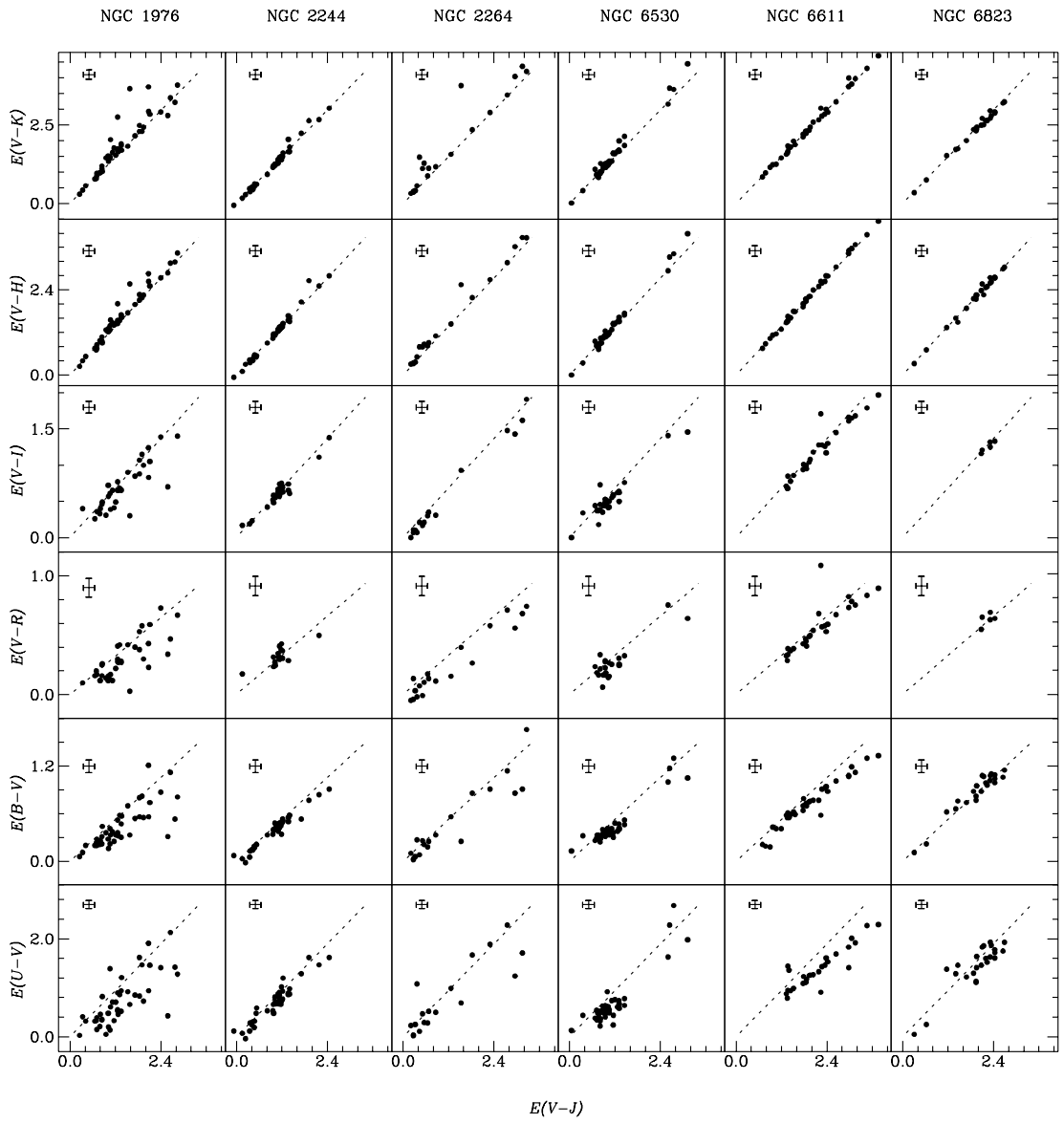

Figure 9. Plots of $E(U-V)$, $E(B-V)$, $E(V-R)$, $E(V-I)$, $E(V-H)$ and $E(V-K)$ against $E(V-J)$. The dotted lines show the reddening vectors characteristic of the normal interstellar extinction law. The length of the crosses represents the observational errors.

differential reddening (Park & Sung 2002), though individual values towards the cluster field range from 0.08 to 0.98 mag (Massey et al. 1995; Berghöfer & Christian 2002). At the time of observations we selected highly probable members based on the study by Marshall et al. (1982), though a recent refined PM study on brighter members (Sabogal-Martínez et al. 2001) dubs many of the high PM members as non-members. In our sample we have stars O I44 (48), O I72 (54), O I91 (59) and O I127 (69) with $E(B-V) \sim 0.05$ mag. We adopt a synthetic $E(B-V)$ of 0.05 and 0.07 mag for stars 48 and 59 as the V magnitude estimates in the literature were highly uncertain and the colour excesses could not be determined in all bands for these stars. A re-estimated PM membership assigns a value less than 0.5 for stars O I72, O I91 and O I127 (Sabogal-Martínez et al. 2001). Similarly the stars O I48 (51), O I78 (55), O I110 (63), O I377 (85) and O I393 (86) have $E(B-V) \sim 0.15$ mag and have low membership according to the new study. Therefore all of these stars were not considered for determining the extinction law for the cluster. On the basis of 11 PM members in Group 1, we determine R_V as 3.16 and a value of $R_V = 3.54$ is obtained on the basis of 18 members in Group 2. Therefore, a significant number of the reddened stars do show anomalous extinction contrary to the earlier finding that the cluster has a normal reddening law, i.e. $R_V \sim 3.2$ (Ogura & Ishida 1981; Park & Sung 2002). The UV extinction properties of eight stars (five O-type, three early B-type) studied by Massa & Conti (1981) suggests cooler UV continua of O-type stars than those of three early B-type stars. However, five of the common O-type stars [O I84(58), O I114(64), O I122(67), O I128(70), O I180(75), O I203(81)] in the current study show normal extinction.

NGC 2264 has the lowest mean reddening, i.e. $E(B-V) = 0.07 \pm 0.03$ mag in our sample (Sung et al. 1997). For stars VAS1 (88), VAS2 (89), VAS11 (91), VAS48 (96) and VAS188 (102), $E(B-V)$ is less than 0.02 mag. The accurate value of R_V for these stars therefore could not be determined. The CEDs have a large scatter with most of them showing peculiar extinction. The remaining stars VAS22 (92), VAS32 (93), VAS86 (99) and VAS192 (103), all of late

Table 9. A comparison of the extinction laws for the programme clusters with the normal interstellar extinction derived theoretically for diffuse dust by van de Hulst (1949) curve No. 15 (see Johnson 1968) and derived observationally by Cardelli, Clayton & Mathis (1989). Columns 4–10 contain mean ± s.e. for the corresponding cluster and group (see Section 4). The asterisked sets of values are derived after subtracting the foreground interstellar reddening (see Section 4.2).

Source Cluster	Groups	No.	$\frac{E(U-V)}{E(V-J)}$	$\frac{E(B-V)}{E(V-J)}$	$\frac{E(V-R)}{E(V-J)}$	$\frac{E(V-I)}{E(V-J)}$	$\frac{E(V-H)}{E(V-J)}$	$\frac{E(V-K)}{E(V-J)}$	R_V
van den Hulst			0.75	0.43			1.13	1.21	
Cardelli et al.			0.78	0.44	0.27	0.56	1.14	1.24	
NGC 1976	1	6	0.80 ± 0.04	0.44 ± 0.01	0.27 ± 0.03	0.57 ± 0.03	1.19 ± 0.02	1.27 ± 0.02	3.18 ± 0.02
	2	28	0.46 ± 0.04	0.29 ± 0.01	0.20 ± 0.01	0.49 ± 0.01	1.19 ± 0.02	1.31 ± 0.02	4.78 ± 0.10
	2*	28	0.45 ± 0.05	0.27 ± 0.01	0.20 ± 0.01	0.48 ± 0.02	1.19 ± 0.02	1.31 ± 0.02	4.90 ± 0.12
NGC 2244	1	11	0.73 ± 0.04	0.42 ± 0.01	0.27 ± 0.01	0.57 ± 0.01	1.11 ± 0.02	1.20 ± 0.01	3.16 ± 0.02
	2	18	0.62 ± 0.01	0.38 ± 0.01	0.27 ± 0.02	0.53 ± 0.01	1.13 ± 0.01	1.23 ± 0.01	3.54 ± 0.04
	2*	18	0.51 ± 0.02	0.35 ± 0.01	0.28 ± 0.03	0.51 ± 0.02	1.13 ± 0.02	1.21 ± 0.02	3.96 ± 0.10
NGC 6530	2	33	0.54 ± 0.02	0.36 ± 0.01	0.23 ± 0.02	0.50 ± 0.02	1.14 ± 0.01	1.25 ± 0.01	3.87 ± 0.05
	2*	33	0.44 ± 0.02	0.32 ± 0.01	0.21 ± 0.03	0.48 ± 0.03	1.13 ± 0.02	1.24 ± 0.02	4.50 ± 0.10
NGC 6611	1	3	0.68 ± 0.01	0.44 ± 0.00	0.25 ± 0.01	0.57 ± 0.03	1.12 ± 0.00	1.22 ± 0.02	3.00 ± 0.02
	2	23	0.63 ± 0.00	0.38 ± 0.00	0.24 ± 0.00	0.54 ± 0.01	1.13 ± 0.01	1.23 ± 0.01	3.56 ± 0.02
	2*	23	0.50 ± 0.02	0.34 ± 0.01	0.22 ± 0.01	0.52 ± 0.01	1.11 ± 0.02	1.23 ± 0.01	4.04 ± 0.03
NGC 6823	1	16	0.70 ± 0.02	0.44 ± 0.01	0.26 ± 0.01	0.56 ± 0.01	1.13 ± 0.01	1.22 ± 0.01	3.04 ± 0.02

spectral type, show abnormal behaviour with a mean $R_V = 3.91 \pm 0.17$. The star W100 (138) show normal behaviour with $R_V \sim 3.03$. Moreover our sample contains a very small number of early-type stars. The abnormal extinction for the late-type stars may also be due to circumstellar material.

In NGC 6530, $E(B-V)$ has a mean of 0.35 mag with abnormal reddening reported for a number of embedded members (van den Ancker et al. 1997; Sung et al. 2000). The star W2 (107) follows normal extinction while a total of 33 stars fall in Group 2 and show abnormal extinction behaviour with $R_V = 3.87 \pm 0.05$. Further support for the anomaly is provided by UV extinction studies (Torres 1987; Boggs & Böhm-Vitense 1989).

NGC 6611 has a mean R_V of 3.75 (3.5–4.8) and $E(B-V)$ of 0.86 mag with variation from 0.4 to 1.8 mag (Hillenbrand et al. 1993). We have also included eight BD stars on the basis of PM data from Kamp (1974); however, five of these stars [BD–134909 (181), BD–134913 (182), BD–144967 (183), BD–144972 (184), BD–144981 (186)] have $E(B-V) \leqslant 0.6$ mag and hence have low membership probabilities. The stars W280 (164), W367 (169) and W412 (171) show the normal law with a mean of $R_V = 3.03$ with the remaining 23 showing abnormal reddening with a mean of $R_V = 3.56$.

NGC 6823 has a mean reddening of $E(B-V) = 0.85$ mag with a range of 0.64–1.16 mag and follows a normal reddening law (Sagar & Joshi 1981; Guetter 1992). The stars 206 and 208 have reddenings of $E(B-V) < 0.22$ mag making them unlikely to be cluster members. The stars E36 (194), E46 (195) and E77 (198) show variability while stars E78 (199), E103 (209) and E110 (211) occupy an anomalous position in the colour–magnitude diagram (Sagar & Joshi 1981). The remaining stars, 16 in total, show a normal reddening with a mean of $R_V = 3.0$, although a closer look at the UBV CEDs may give the impression that the cluster region contains material representing a shallower as well as a steeper R_V than the ISM. This aspect requires further investigation.

Using data from highly reddened stars with no emission features and high membership probabilities (i.e. Group 1 + Group 2 stars), the clusters present diverse extinction properties. The clusters NGC 6530 and NGC 6823 are represented by single extinction laws with the value of R_V 3.87 ± 0.02 and 3.00 ± 0.02, respectively. A small fraction of the stars (18, 37 and 14 per cent, respectively) in the clusters NGC 1976, 2244 and 6611 show normal extinction with R_V equal to 3.18 ± 0.02, 3.16 ± 0.02 and 3.00 ± 0.02, respectively, while the major fraction of stars show anomalous extinction with the corresponding R_V of 4.78 ± 0.10, 3.54 ± 0.04 and 3.56 ± 0.02, respectively. It should be noted that the anomalies in colour excess ratios and the value of R_V for four clusters (see Table 9) is derived from a combination of interstellar reddening and cluster or circumstellar matter, the properties of which may not be identical. Therefore, a constant interstellar reddening corresponding to the cluster minimum ($E(B-V) = 0.05$, 0.20, 0.15 and 0.40 mag for clusters NGC 1976, NGC 2244, NGC 6530 and NGC 6611, respectively) was subtracted from the global reddening and the colour excess ratios were derived again for these clusters. The values obtained in this way are listed in Table 9 (asterisked set). The effect is smaller for NGC 1976 as it has a small foreground reddening, but it is more for other clusters. For example the abnormal value of $R_V = 4.8$ derived by Chini & Wargau (1990) is comparable to 4.04 in the case of NGC 6611. We could not derive a representative value of R_V for NGC 2264 due to small statistics. The clusters NGC 2264 and NGC 1976 have the largest scatter in the value of R_V, i.e. from 2.8 to 6.7 and from 3.07 to 9.9, respectively. The above observations based on reddened members led us to conclude that the young clusters, four out of six, appear to have anomalous extinction in general, indicating the prevalence of larger than normal grain size dust distributions in the star-forming regions. This supports the earlier finding of steeper R_V than for the ISM in star-forming regions (Terranegra et al. 1994). The mean normal value of R_V for the clusters NGC 1976 and NGC 2244 (with distances $D < 2$ kpc) is 3.17 ± 0.03 while for the clusters NGC 6611 and NGC 6823 ($D > 2$ kpc), $R_V = 3.01 \pm 0.03$. These figures are in excellent agreement with the distance dependence of R_V for the diffuse dust reported in the literature (see table 5 of He et al. 1995). This indicates that the early-type stars with high $E(B-V)$ do provide a reliable estimate of R_V.

5 INFRARED PROPERTIES

5.1 NIR excess

The interstellar as well as intracluster material show normal reddening for wavelengths $\lambda \geqslant \lambda_J$ irrespective of the grain properties of the matter. Therefore the nature of extinction due to circumstellar material can be indicated by an excess or a deficit of radiation at wavelengths longward of 1 μm. In order to probe this aspect, we derive $V - H$ and $V - K$ colour excesses individually for all programme stars from the colour excess $E(V - J)$ assuming a normal extinction law. The differences between these and the observed colour excesses derived on the basis of the spectra are plotted in Fig. 10 and show a random scatter around the mean indicating the independence of the extinction at J. The scatter is best represented by the average values of 0.02 ± 0.09 (s.d.) mag for $\Delta(V - K)$ and 0.01 ± 0.07 (s.d.) mag for $\Delta(V - H)$. These estimates were determined by ignoring highly deviant points and are based on 195 and 204 data points in H and K, respectively. We expect the star to have a NIR excess if it has differences greater than 2σ at either H or K or at both. There are 10, 11 and 20 stars which have differences $>5\sigma$, 3–5σ and 2–3σ, respectively, at either H or K or both. Table 10 provides a list of all these stars with their differences. Several of these stars are reported to have large or moderate NIR excess, e.g. for stars 5, 8, 14, 24, 27 and 33 by Qian & Sagar (1994); for stars 160 and 175 by Hillenbrand et al. (1993); for stars 115, 122, 136, 149 and 151 by van den Ancker et al. (1997). Stars 17, 18, 119, 194, 198 and 133 also show a NIR deficiency at H or K or both.

Table 10. Near-IR flux excess and deficiency. Δ represent differences in the spectral type calibrated colour excess and the normal reddening-based colour excesses estimated using $E(V - J)$, e.g. $\Delta(V - H) = E(V - H)_{\rm Normal} - E(V - H)_{\rm SpT}$.

ID	$E(V-J)$	Δ		ID	$E(V-J)$	Δ	
		$(V-H)$	$(V-K)$			$(V-H)$	$(V-K)$
5	1.07	0.33	0.70	94	3.15	0.29	0.45
6	0.95	0.19	0.27	95	2.96	0.25	0.37
8	1.26	0.57	1.19	97	1.53	0.81	1.85
12	2.11	0.10	0.22	98	0.43	0.30	0.94
14	1.84	0.17	0.20	100	0.51	0.21	0.48
17	2.77	0.03	−0.21	101	0.56	0.23	0.59
18	2.58	−0.06	−0.40	109	0.82	0.11	0.25
22	1.35	0.15	0.22	115	3.12	0.43	0.57
23	1.35	0.16	0.17	119	0.77	−0.16	−0.12
24	2.08	0.27	0.35	122	1.31	0.14	0.37
27	2.07	0.50	1.14	126	1.45	0.09	0.33
29	1.06	0.18	0.17	133	0.94	0.17	0.09
31	1.12	0.19	0.23	136	0.67	0.19	0.26
32	1.16	0.09	0.32	149	2.13	0.25	0.33
33	1.01	0.07	0.26	151	2.75	0.29	0.22
35	1.58	0.77	1.69	160	2.98	0.11	0.29
36	2.84	0.20	0.25	175	2.24	0.09	0.25
82	1.37	0.11	0.34	194	1.46	−0.17	−0.07
87	1.91	0.48	0.26	198	2.14	−0.18	−0.14
90	3.26	0.15	0.16	209	2.10	0.18	0.11
92	0.68	0.13	0.28				

5.2 Dereddened colour–colour diagram

In order to understand the nature of the NIR excess we generate the dereddened colour–colour [$(J - H)_0$ versus $(H - K)_0$] diagram. For this we chose $E(V - J)$ to estimate A_V($\sim$ 1.1 $E(V - K) \sim$ 1.364 $E(V - J)$ – assuming normal reddening) for stars showing an NIR excess (see Section 4.1 for detailed discussion). The colour excesses $E(J - H)$ and $E(H - K)$ were derived as $0.11A_V$ and $0.065A_V$, respectively (Rieke & Lebofsky 1985). The typical uncertainty in these colours is ∼0.1 mag with a maximum up to 0.15. The dereddened NIR colour–colour diagram is shown in Fig. 11 and is used to identify non-MS stars and their nature in combination with the spectral properties.

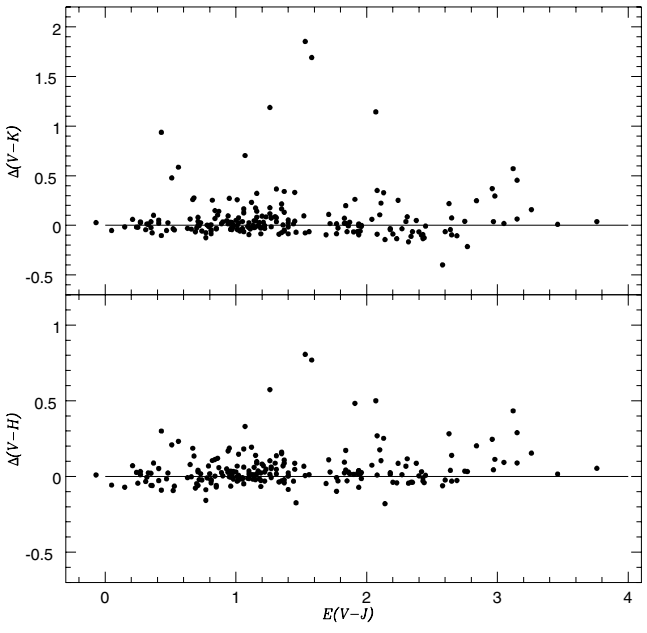

Figure 10. Plots of $\Delta(V - K)$ and $\Delta(V - H)$ against the colour excess $E(V - J)$. Horizontal lines denote zero-level differences.

Most of the 14 stars showing only Balmer emissions are of early type (F0) except star 92 which is of F8 type, and occupy positions towards the right of the reddened MS and possess moderate to strong NIR excesses. These are probable HAB or classical Be stars. Four of these stars (8, 35, 97, 98) have strong NIR excesses and lie to the extreme right in the colour–colour diagram. These are late B- or early A-type stars and appear to show Group I HAB characteristics (Hillenbrand et al. 1992, 1993), while another group of five stars (109, 122, 126, 160, 175) have moderate NIR excesses and lie isolated towards the right and lower down in the diagram. These early-type stars ($\leqslant$B5) are possible Group II or III HAB candidates. Two of these stars (160, 175) have rigorously been argued to have HAB characteristics and were kept in Group III by Hillenbrand et al. (1993). A further group of four stars (22, 115, 173, 174) shows weak emission features and lie within the reddened MS region; these are probably so-called classical Be stars. The list of these 13 probable PMS or Be stars is given in Table 11.

A group of 18 late-type stars ($\geqslant$F8) are probable T Tauri stars (see Table 12). Six of these stars (5, 27, 32, 33, 100, 101) have high to moderate NIR excesses and Hα emission above the continuum with a mean EW of $\sim$ 5 Å. In the $(J - H)_0$ versus $(H - K)_0$ diagrams they occupy a position just below the zero-age main-sequence (ZAMS) track of classical T Tauri (CTT) stars. These stars have both Ca II HK and Balmer lines in emission. Moreover, star 27 also has Paschen-line emission; stars 27 and 33 have emission-like spectra; star 33 has strong Li absorption while stars 27 and 32 are reported to vary in the NIR. Therefore these stars appear to have the characteristics of CTT stars. Another group of 12 stars (6, 15, 23, 29,

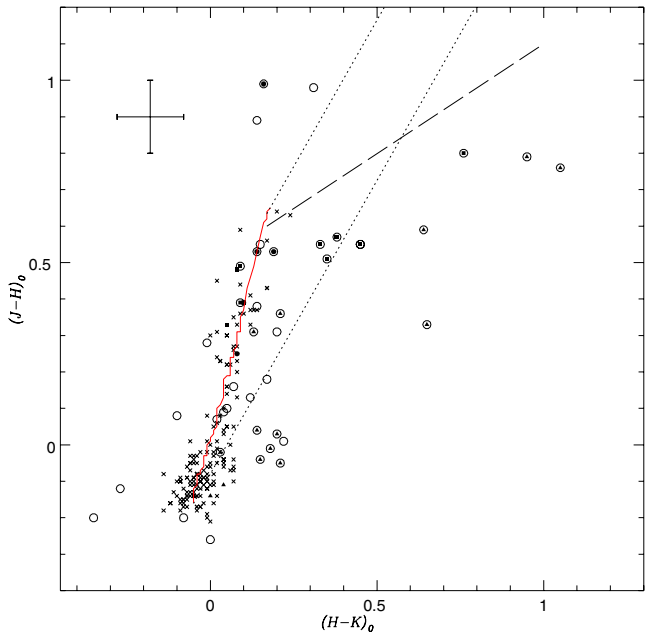

Figure 11. The dereddened colour–colour diagram for all the programme stars. Crosses denote normal stars with no NIR and spectral peculiarities while the filled triangles, filled squares and filled circles denote stars with Balmer emissions, with H I+Ca II HK and with Ca II HK emissions, respectively. The circling around these symbols or an open circle denote NIR excess or deficiency. The solid line traces the ZAMS stars up to M0 while the dotted lines are normal reddening line and correspond to $E(J-H)/E(H-K) = 1.7$ (Rieke & Lebofsky 1985). The dashed line represents the locus of CTT stars (Meyer, Calvet & Hillenbrand 1997).

31, 34, 53, 90, 91, 92, 99, 178) occupy the location of weak-line T Tauri (WTT) stars. Six of these show weak excesses and the rest do not show any excess. Two of them (92 and 99 – both F8) probably belong to the post-T Tauri phase and are about to reach the ZAMS.

The stars 87, 149 and 151 are either giants or supergiants of K spectral type. Star 87 also shows Ca II HK emissions and moderate IR excess while star 151 is a variable (Sagar & Joshi 1978) and shows strong IR excess. Their distinct location a little to the left and above the reddened MS suggests that these may be supergiants. In fact two of these stars (149, 151) have been reported in the literature as probable post-asymptotic giant branch (AGB) candidates (van den Ancker et al. 1997).

5.3 Spectral energy distributions

The presence of circumstellar material, their geometry and the nature of radiation is best studied by spectral energy distributions (SEDs) covering the MIR region. The SEDs are derived using reddening-corrected broad-band fluxes. The reddened broad-band optical and NIR fluxes were taken from Table 4 while MIR fluxes are taken from Table 5. The dereddened fluxes were derived using R_V-dependent analytical expression given by Cardelli et al. (1989). The values of $T_{\rm eff}$ (effective temperature) and $\log(g)$ (gravity) corresponding to the adopted spectral type are taken from Schmidt-Kaler (1982). The reddened, dereddened and synthetic KURUCZ (1993) spectra based on $T_{\rm eff}$ and $\log(g)$ were plotted and found to match in all cases, authenticating the determination of temperature, gravity and reddening. Fig. 12 provides these plots for stars having fluxes in MIR bands. The synthetic spectra are normalized in the V band. The MIR region contains fluxes in six bands (7, 12, 15, 25, 60, 100 μm). Of 65 stars with MIR fluxes, 32 have fluxes in more than two bands while another 13 have fluxes in two bands only. We determined the spectral index s, defined as $\lambda\ F_\lambda \sim \lambda^s$, in the region 2.2–25 μm as most of the known *IRAS* fluxes at 60 and 100 μm are only upper limits. The value of s is listed in Table 5. It is seen that 17 stars have a value of s close to −3.0, representing a blackbody. Another group of 17 stars have fluxes only at one, two or three bands but their s values deviate significantly; however, these determinations may be considered uncertain. The remaining 31 stars have fluxes at more that three MIR bands and may be considered a reliable determination of spectral index (Table 5). The values of s, if available, deviate significantly from blackbodies for the probable PMS stars with circumstellar material (Table 12). In addition, there is a group of MS and post-MS stars which also appears to deviate from blackbodies and are considered to be probable candidates with circumstellar material. The list of these stars, 37 in total, is provided in Table 12.

6 EVOLUTIONARY STATUS AND NATURE OF INDIVIDUAL STARS

The luminosity was derived using $\log(L/\ {\rm L}_\odot = 1.9\text{–}0.4\ M_{\rm bol})$, where $M_{\rm bol}$ is written as $M_J + (V-J)_0 + {\rm BC}_V$. The value of BC_V is taken from Code et al. (1976), Bessell & Brett (1988) and Massey, Parker & Garmany (1989). M_J is derived using the cluster distances as given in Table 1 and A_J is given as $0.28\ A_V$. The uncertainty in luminosity is mainly contributed by uncertainty in the J magnitude apart from the uncertainties in bolometric corrections, distances and extinction. All added together amount to a maximum uncertainty of ∼0.06 in $\log(L)$. The uncertainties in $\log(T_{\rm eff})$ are generally below 0.02. The Hertzsprung–Russell diagram (HRD) of all the programme stars is shown in Fig. 13. The selected clusters have a PMS (turn-on) age in the range 1–3 Myr and age spreads ∼8 Myr (see Table 1), where PMS age denotes the median value of the age distribution of individual stars while the value of age spread contains 95 per cent of the stars in the cumulative age distribution (Park et al. 2000). The turn-on ages usually agree with the turn-off ages and provide clues to the duration of star formation. The derived PMS age and, in particular, the age spread, depends on the treatment of convection and opacity in stellar atmospheres and is found to vary widely from model to model (see Hartigan, Strom & Strom 1994; Park, Sung & Kang 2002; Wolff, Strom & Hillenbrand 2004). We have chosen the frequently used PMS tracks by D'Antona & Mazzitelli (1994) as none of our stars have masses below 1 $M_\odot$. In the HRD of sample clusters, the stars with masses $\geqslant 3\ M_\odot$ are on the MS whereas the low-mass stars (<2 –3 $M_\odot$, i.e. ∼25 per cent of the sample) are still in their PMS stage. In the present sample, most of the identified PMS stars lie around the 2-Myr evolutionary track and are below the birth-line (Fig. 13); however, some of the stars are non-members and lie above the birth-line. The spread seen in the MS is probably due to the effect of binarity, variability and uncertainty in the flux conversions rather than the real evolutionary effects on the MS. The HRDs of the clusters have been used to infer the nature and evolutionary status of individual stars as described below.

6.1 Clusters

NGC 1976 is an open cluster with a high proportion of low-mass stars, a median age ∼1 Myr and an age spread ∼8.5 Myr as derived from PMS stars (Park et al. 2002). Fifty-five to 99 per cent of the low-mass stars in NGC 1976 are found to have circumstellar discs from NIR data by Hillenbrand et al. (1998). Our sample contains

Table 11. List of probable PMS stars with circumstellar material. The letters Y and N stands for 'yes' and 'no', respectively, in columns 4, 5 and 9 while the letters W, M and S in column 6 denote weak (2–3σ), moderate (3–5σ) and strong (>5σ) excesses, respectively (see Section 5.1). Stars with a plus symbol are reported to show variability at optical wavelengths. The MIR spectral index (SpI), s (i.e. $\lambda F_\lambda \sim \lambda^s$), is given in column 8. The nature of the star, i.e. classical Be (CBe), Herbig Ae/Be (HAB) and their groups (see Section 5.2), classical T Tauri (CTT) and weak line T Tauri (WTT) is given in the last column.

ID	Cluster ID	SpT	H I	Ca II	Excess (NIR)	EW (Hα) (Å)	SpI (s)	Memb	Remark
5+	NGC 1976 P1409	F8 V	Y	Y	S	−4.0	-0.79 ± 0.01	Y	CTT
6	NGC 1976 P1469	G9 IV–V	–	Y	W	–	–	Y	WTT
8	NGC 1976 P1623	A2 e	Y	–	S	1.6	–	Y	HAB I
15+	NGC 1976 P1799	K0 V	–	Y	–	–	–	Y	WTT
22	NGC 1976 P1891	O7	Y	–	W	–	–	Y	CBe
23	NGC 1976 P1955	G0 III–IV	Y	Y	W	–	–	Y	WTT
27+	NGC 1976 P2029	G3 IV–V	Y	Y	S	−7.0	0.52 ± 0.10	Y	CTT
29	NGC 1976 P2069	G8 V	Y	Y	W	–	–	Y	WTT
31	NGC 1976 P2100	G9 IV–V	–	Y	W	–	–	Y	WTT
32+	NGC 1976 P2115	K2 IV	Y	Y	M	−4.1	–	Y	CTT
33+	NGC 1976 P2181	K2 V	Y	Y	W	−3.0	–	Y	CTT
34	NGC 1976 P2244	K1 V	Y	Y	–	–	–	Y	WTT
35+	NGC 1976 P2247	A3 e	Y	–	S	−3.0	–	Y	HAB I
91	NGC 2264 VAS11	G0	–	Y	–	–	–	Y	WTT
92	NGC 2264 VAS22	F8	Y	–	W	–	–	Y	WTT
97+	NGC 2264 VAS62	B8 e	Y	–	S	−14.7	0.30 ± 0.17	Y	HAB I
98+	NGC 2264 VAS72	A2 IVe	Y	–	S	0.2	−1.20	Y	HAB I
99	NGC 2264 VAS86	F8 V	Y	Y	–	–	–	Y	WTT
100+	NGC 2264 VAS92	G5 V	Y	Y	S	−4.3	–	Y	CTT
101+	NGC 2264 VAS122	G8 V	Y	Y	S	−2.1	1.54 ± 0.43	Y	CTT
109	NGC 6530 W5	B5	Y	–	W	–	0.77	Y	HAB I or III
115	NGC 6530 W29	B2	Y	–	W	–	–	Y	CBe
122	NGC 6530 W58	B2 V	Y	–	M	–	–	Y	HAB I or III
126	NGC 6530 W65	B0 IV	Y	–	M	–	-0.10 ± 0.58	Y	HAB I or III
160	NGC 6611 W235	B2	Y	–	M	–	−2.30	Y	HAB III or CBe
173	NGC 6611 W469	B0.5	Y	–	–	–	0.61 ± 0.34	Y	HAB I or III
174	NGC 6611 W483	B5	Y	–	–	–	–	Y	CBe
175	NGC 6611 W503	B1	Y	–	W	–	-0.47 ± 0.59	Y	HAB I or III

19 stars with masses ranging from 1 to 3 $M_\odot$ and ages from 1 to 3 Myr except stars P1360 (4), P1699 (10), P2317 (38) and P2367 (39) which have low luminosity and show ages ∼10 Myr. The latter are PM members with R_V typical for NGC 1976 and have masses below 1.5 $M_\odot$ with no PMS characteristics. Therefore, these are probably in the post-T Tauri phase with a nearly edge-on disc (Park et al. 2002). Eleven of these stars show PMS characteristics. The stars P1409 (5), P2029 (27), P2115 (32) and P2181 (33) show CTT characteristics as is seen from the strong NIR excesses, their location in the dereddened NIR colour–colour diagram (as all of them lie along the CTT loci), Hα emission (EW ∼6 Å) and a circumstellar disc as seen from the Ca II T linewidths. These are identified as PMS objects in the literature. The stars P1469 (6), P1736 (12), P1799 (15), P1955 (23), P2069 (29), P2100 (31) and P2244 (34) have weak NIR excess, low or absent emission activities and some show light variability in the NIR suggesting that these are WTT stars, though a further investigation is needed to know their true nature. The Ca II T measurements for stars P1469 and P1955 indicate that they have a weak accretion disc, supporting the recent finding by Littlefair et al. (2004) that WTT stars also possess accretion discs, contrary to the earlier conception that they are non-accreting discless objects. A recent PM study by Tian et al. (1996) makes star P1469 a non-member (zero probability of membership) whereas the star has weak NIR excess, shows Ca II emission and is variable in NIR light (Carpenter 2001), suggesting that it is a PMS object. The stars P1469, P1799, P1955 and P2069 are reported to show emission features for the first time. Another group of three intermediate-mass stars [P1623 (8), P1891 (22), P2247 (35)] show PMS characteristics and probably belong to the HAB group. Star 35 is a well-known HAB star (Hillenbrand et al. 1992; Herbig 1994; Leinert, Richichi & Haas 1997; Maheswar, Manoj & Bhatt 2002). The stars P1623 and P1891 have Hα filled-in with emission and show weak NIR excesses. As star P1623 is located very close to star P2247 in the HR diagram and is of early A type, it is most likely a HAB star. Further study is required to probe the true nature of stars P1623 and P1891. The remaining group of 22 stars lies on the MS. Of these, stars P1044 (1), P1736 (12), P1772 (13), P1798 (14), P1956 (24), P2074 (30), P2248 (36) and P2425 (41) are found to have circumstellar material as is seen either from a weak NIR excess or above-zero value of the MIR spectral index, s. The mean value of s for these stars is above zero, suggesting that they contain cool circumstellar dust. These are probable Vega-like stars or are precursors to such a phenomenon. The Vega-like stars are characterized by substantial far-infrared excesses due to cool dust, relatively low NIR excesses, low polarization and a lack of emission lines in their spectra. In fact, one of these stars (P1772) has recently been studied in detail and was identified to have Vega-like characteristics by Manoj, Maheswar & Bhatt (2002).

NGC 2244 is a young cluster and recent studies suggest on-going star formation in the region (Pérez 1991; Berghöfer & Christian 2002). It has a median PMS age ∼1.9 Myr and an age spread of ∼6 Myr (Park & Sung 2002). Though Massey et al. (1995) suggest the existence of intermediate-mass PMS stars, a recent study by Park & Sung (2002) found a gap near 2 $M_\odot$, and the most massive

Table 12. List of probable non-emission MS and post-MS stars with circumstellar material. The letters Y, PY and N in column 6 stands for 'yes', 'probably yes' and 'no', respectively, while the letters W, M and S in column 4 denote weak (2–3σ), moderate (3–5σ) and strong (>5σ) excesses, respectively. Asterisked star have Ca II HK in emission and stars with the plus symbol are reported to show variability at optical wavelengths. The mid-IR spectral index (SpI), s (i.e. $\lambda F_\lambda \sim \lambda^s$), is given in column 5. The last column gives the type of star; 'PVLS' stands for probable Vega-like star.

ID	Cluster ID	SpT	Excess (near-IR)	SpI (s)	Memb	Remarks
1	NGC 1976 P1044	B2.5 IV	–	-0.42 ± 0.74	Y	PVLS
12	NGC 1976 P1736	F8	W	–	Y	PVLS
13	NGC 1976 P1772	B2 V	–	1.44 ± 0.25	Y	PVLS
14	NGC 1976 P1798	B3 V	W	–	Y	PVLS
24+	NGC 1976 P1956	B2 V	W	–	Y	PVLS
30	NGC 1976 P2074	B0.5 V	–	0.85 ± 0.24	Y	PVLS
36	NGC 1976 P2248	B4 V	W	0.14 ± 0.37	Y	PVLS
41	NGC 1976 P2425	B5 V	–	0.14 ± 0.05	Y	PVLS
54	NGC 2244 O I72	F4	–	0.72 ± 0.53	N	PVLS
57	NGC 2244 O I80	B0.5 V	–	-0.55 ± 0.13	Y	
60	NGC 2244 O I102	F7	–	0.65 ± 0.37	PY	PVLS
62	NGC 2244 O I109	A5	–	1.24 ± 0.50	Y	PVLS
65	NGC 2244 O I115	B0 V	–	-0.96 ± 0.48	Y	
71	NGC 2244 O I130	B2.5 V	–	0.36 ± 0.12	Y	PVLS
82	NGC 2244 O I253	B3 V	M	–	Y	
87*	NGC 2244 O I397	K3 Ib	S	-2.55 ± 0.13	PY	AGB ?
94	NGC 2264 VAS46	B3 V	W	–	Y	PVLS
95	NGC 2264 VAS47	B2 V	W	–	Y	VLS
110	NGC 6530 W7	O4 V	–	-0.09 ± 0.10	Y	
111	NGC 6530 W9	B0 V	–	0.50 ± 0.47	Y	PVLS
119	NGC 6530 W43	B2 V	–	0.12 ± 0.41	Y	PVLS
121	NGC 6530 W56	B1.5 V	–	0.80 ± 0.23	Y	PVLS
129	NGC 6530 W73	B2 IV	–	0.24 ± 0.42	Y	PVLS
134	NGC 6530 W85	B0.5 V	–	-0.08 ± 0.22	Y	PVLS
136	NGC 6530 W93	B2 IV	W	–	Y	PVLS
146	NGC 6530 VA107	B2	–	2.80 ± 0.16	Y	PVLS
149	NGC 6530 VA304	K7 III	M	-2.78 ± 0.15	PY	AGB ?
151+	NGC 6530 VA338	K7 III–IV	M	-2.79 ± 0.40	PY	AGB ?
154	NGC 6611 W161	O5.5 V	–	0.59 ± 0.12	Y	PVLS
166	NGC 6611 W306	B1.5 V	–	1.46 ± 0.27	Y	PVLS
172	NGC 6611 W468	B1 V	–	0.06 ± 0.38	Y	PVLS
179	NGC 6611 K601	B1.5 V	–	-0.62 ± 0.96	Y	
188	NGC 6823 E4	B0.5 IV	–	-0.33 ± 0.09	Y	
200	NGC 6823 E80	B2.5 V	–	-1.36 ± 0.63	Y	
203	NGC 6823 E84	B0.5 V	–	-1.64 ± 0.79	Y	
204	NGC 6823 E86	B0.5 V	–	-1.89 ± 0.24	Y	
210	NGC 6823 E104	B0.5 V	–	0.16 ± 0.21	Y	PVLS

PMS stars reported are of spectral type G2. Our sample contains 16 stars of spectral type later than A0; many of these are non-members as judged by more than one membership indicator supporting the scarcity of PMS objects near A0. The stars O I44 (48), O I48 (51), O I72 (54), O I78 (55), O I91 (59), O I110 (63), O I127 (69) and O I393 (86) are non-members (see Section 4.2). The stars O I29 (47), O I63 (53), O I102 (60) and O I377 (85) are PM members but their locations in the HR diagram suggest them to be non-members. Moreover, the star O I102 has a value of $s \sim 0.45$ indicating that it is surrounded by cold circumstellar material, therefore it may also be a candidate PMS star. The stars O I14 (45) and O I20 (46) are PM non-members while the stars O I109 (62) and O I397 (87) appear to be members. The star O I109 is probably an early A-type Vega-like MS star with cool circumstellar dust as indicated by the index s, while star O I397 is probably a red-supergiant with mass $\sim$12 $M_\odot$ and age $\sim$20 Myr. The remaining group of 28 stars is probably on the MS with masses in the range 3 -80 $M_\odot$. Of these, star O I130 (71) shows Vega-like characteristics.

Being a nearby cluster, NGC 2264 harbours a number of peculiar stars and has frequently been used to test PMS evolutionary models, to study the initial mass function (IMF) and to understand the role of stellar variability in stellar evolution (Walker 1956; Kippenhahn 1965; Flaccomio et al. 1999; Park et al. 2000, 2002; Rebull et al. 2002). It is observed to have an age of $\sim$1.5 Myr and age spread $\sim$9 Myr. Our sample contains 19 stars and most of them are of spectral type A0 and later. The identified PMS stars [VAS22 (92), VAS86 (99), VAS92 (100), VAS122 (101)] do lie in the expected age range. The star VAS11 (91) lies on the ZAMS and shows Ca II HK in weak emission, therefore it is probably a foreground MS star or a BMS (below or near ZAMS) star in the post-T Tauri phase. The BMS stars are T Tauri stars with nearly edge-on discs which obscure the light from the central star and makes them low luminosity. Observations indicate that $\sim$3–5 per cent of the stars with discs are edge-on systems (Park et al. 2002). The star VAS10 (90) shows light-variability and is a field star. The stars VAS32 (93), VAS192 (103), VAS228 (105) and VAS238 (106) lie above

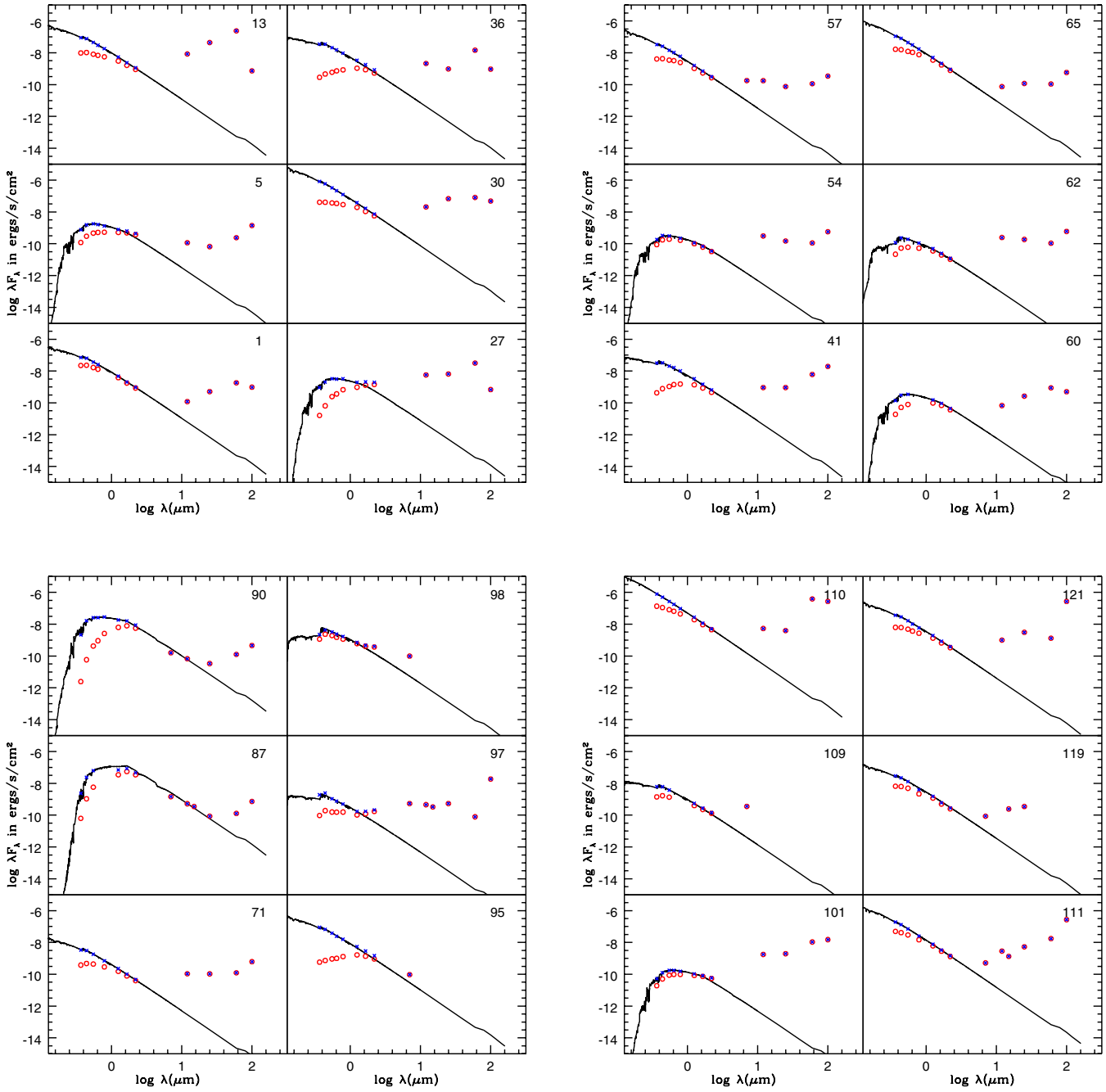

Figure 12. Observed (open squares) and extinction-free (crosses) SEDs of programme stars. The solid lines represent the model SEDs from Kurucz (1993) as expected from the intrinsic properties of the star. The model SEDs are adjusted to coincide at *V* wavelength.

the birth-line and have a large value of $E(B-V)$, therefore they are probably background non-members. The star VAS227 (104), of A type, also appears to be a foreground non-member located far below the ZAMS. Among the intermediate-mass objects, stars VAS62 (97) and VAS72 (98) are reported to be PMS candidates (Sung et al. 1997; Park et al. 2002). These are HAB stars. The stars VAS46 (94) and VAS47 (95) have weak NIR excesses and are located on the MS, therefore we consider them as candidates for Vega-like cluster members.

Star formation and PMS stars in NGC 6530 have been studied in detail by van den Ancker et al. (1997) and by Sung et al. (2000). It has a PMS age of ∼1.5 Myr with an age spread of ∼5 Myr. In the HR diagram, the stars W35 (117), VA92 (143), VA97 (145), VA304 (149) and VA338 (151) are located well above the birth-line and are foreground non-members, though stars VA304 and VA338 are more luminous, show NIR excesses and are reported to be probable post-AGB candidates (van den Ancker et al. 1997). The star VA338 also shows light variability. The post-MS track for a 12 - $M_\odot$ star appears to follow their location in the HR diagram. These, as well as the star O I397 (87) in NGC 2244, occupy red-giant branch (RGB) locations in the HR diagram; however, a 10 - $M_\odot$ evolutionary track would place them in an AGB phase pushing the age a little older to ∼30 Myr. So, the indicators do support these being cluster members in either RGB, AGB or post-AGB phases. Massive AGB stars in

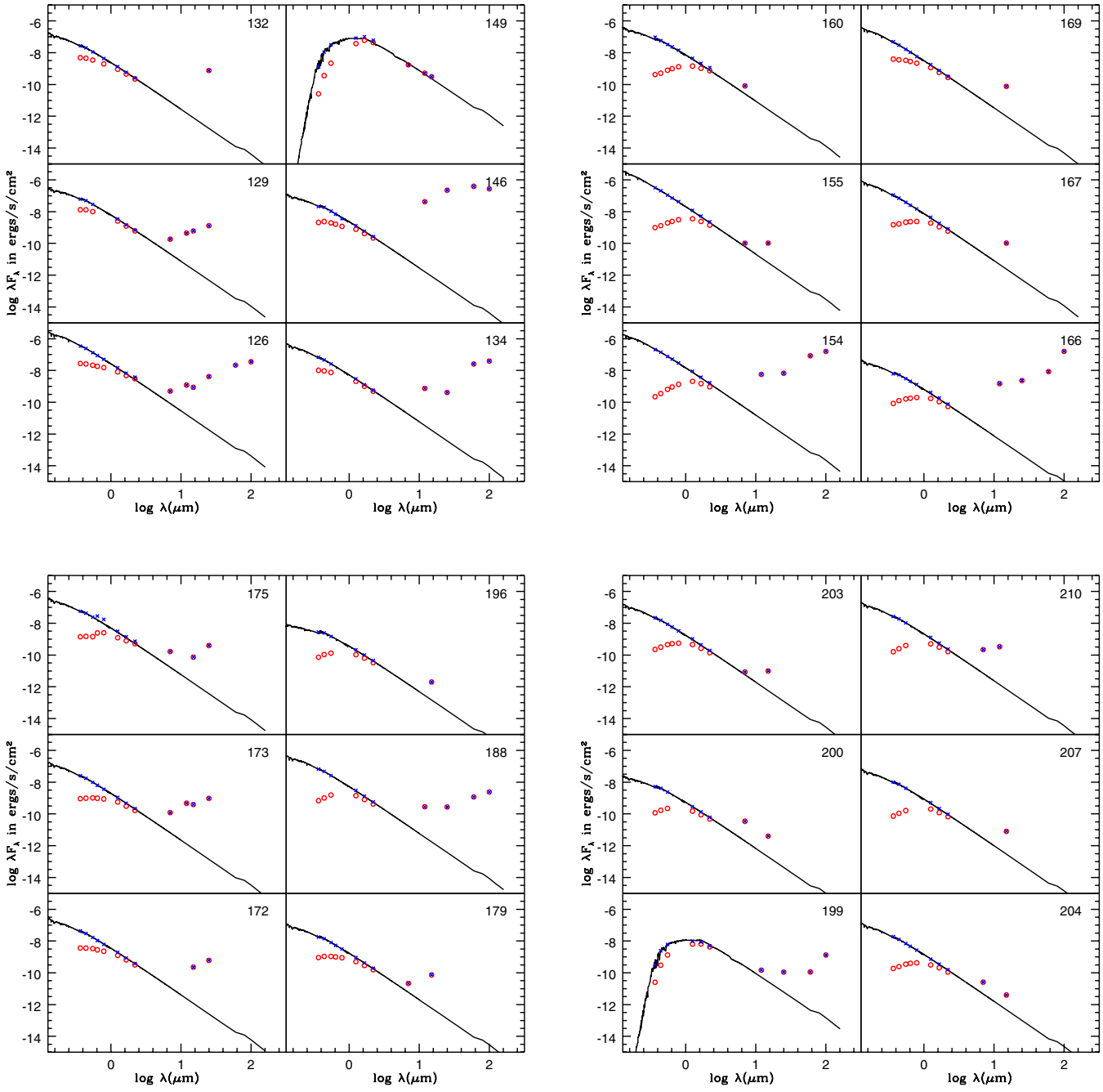

Figure 12 – *continued*

the Galaxy and the Magellanic Clouds are extremely long-period Miras. In the Magellanic Clouds they have invariably shown s-process enhancements and nitrogen overabundances. Luminous red giants without s-process enhancements are more likely to be red supergiants (Wood, Bessell & Fox 1983) and moreover red supergiants are found to exist in young clusters in the Magellanic Clouds (Keller 1999; Keller, Bessell & Da Costa 2000). On the other hand, the resulting distance modulus corresponding to the absolute magnitude of a K-type supergiant star is in agreement with the cluster distances. If this scenario is true for clusters NGC 2244 and 6530 then these are the stars formed ∼20–30 Myr ago, extending the duration of star formation to a few tens of Myr, although a detailed spectroscopic investigation is needed to confirm the nature of these stars. The star W27 (114) is a foreground giant with a very low $E(B-V)$. Among the remaining objects, stars W5 (109), W29 (115), W58 (122) and W65 (126) have weak to moderate excesses and show Hβ in emission. Moreover, the stars W9, W58 and W65 also occupy separate positions in the dereddened NIR colour–colour diagram. They are probable Group II HAB stars as the values of s for star W5 and W65 are above or near zero. Star W58 is suggested to be a HAB star by Boesono, Thé & Tjin A Djie (1987). The location of star W29 in the NIR colour–colour diagram indicates that this is a Be star candidate. Another group of eight stars [W7 (110), W9 (111), W43 (119), W56 (121), W73 (129), W85 (134), W93 (136), VA107 (146)] show Vega-like characteristics mostly showing substantial MIR excesses.

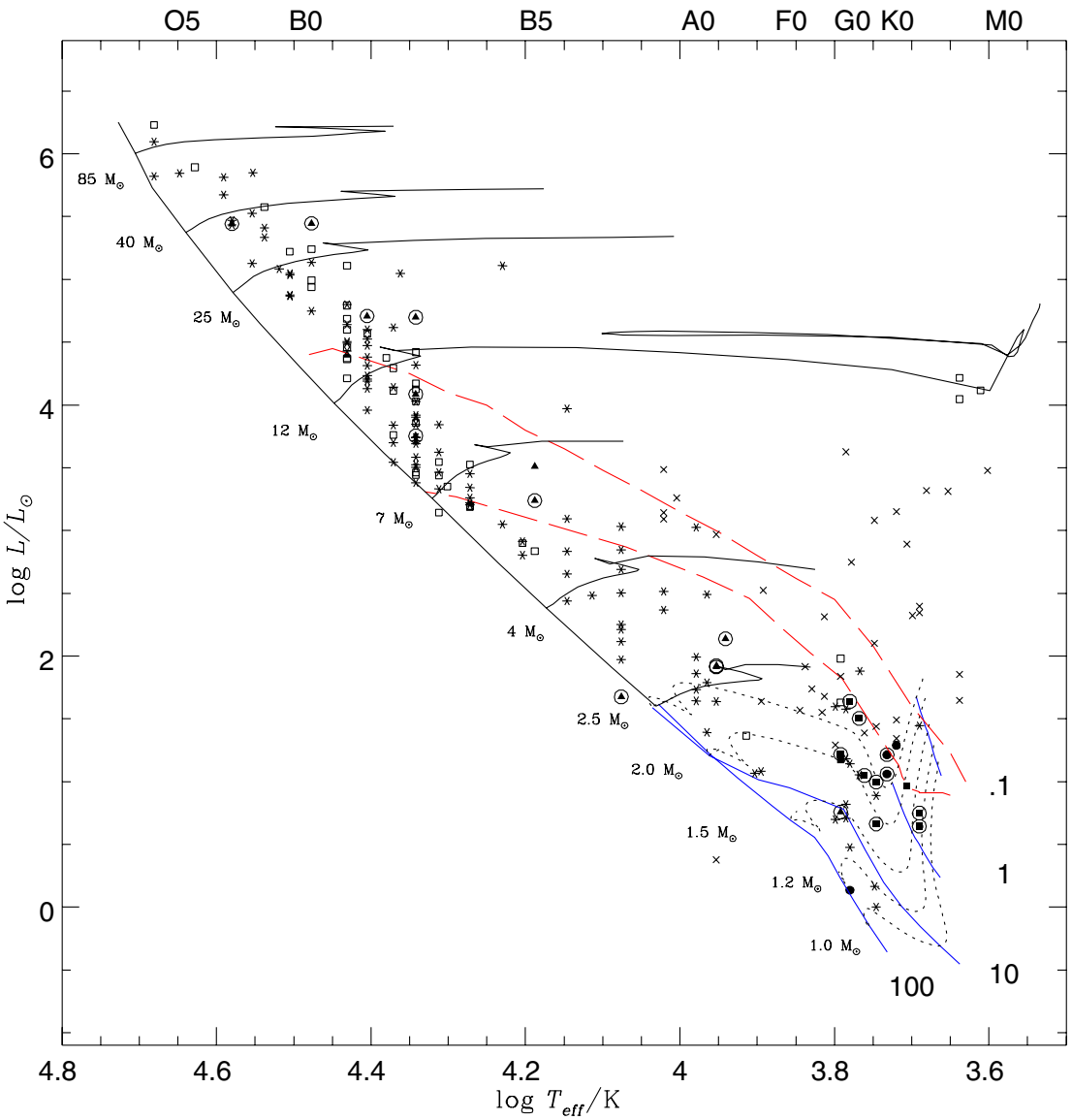

Figure 13. The theoretical HR diagram of all the programme stars. Stars finally rejected from the membership are denoted with crosses. A group of 28 probable Herbig Ae/Be, classical Be or T Tauri population is shown by filled triangles, filled squares and filled circles representing stars with H I (Balmer), with H I+Ca II HK and with Ca II HK emissions, respectively (see Tables 7 and 11). The circling around these symbols denote NIR excess. The asterisks denote normal stars while the open squares represent stars with circumstellar material as seen from either MIR spectral indices or NIR excesses or from both (see Tables 10 and 12). The dotted lines show PMS evolutionary tracks (1.0, 1.2, 1.5, 2.0, 2.5 $M_{\odot}$) along with the isochrones (solid lines) for 0.1, 1, 10 and 100 Myr which are taken from D'Antona & Mazzitelli (1994). The upper and lower dashed lines represent birth-lines corresponding to the accretion rates 10^{-4} and 10^{-5} $M_{\odot}$ yr^{-1}, respectively, and are taken from Palla & Stahler (1993). The ZAMS and post-MS evolutionary tracks (85, 40, 25, 12, 7, 4 and 2.5 $M_{\odot}$) are shown with solid lines and are taken from Schaller et al. (1992).

NGC 6611 is also well studied and is reported to contain hundreds of low-mass PMS stars with a median age of ∼2 Myr and an age spread ∼7 Myr (Hillenbrand et al. 1993; Belikov et al. 2000). In the HR diagram, the stars K576 (177), K599 (178) and BD–144974 (185) lie well above the birth-line and have $E(B-V) < 0.6$ mag, lower than the cluster mean ∼0.86 mag. A recent PM study by Belikov et al. (1999) assigns proper-motion membership, $P_{\mu} = 0.08$, for star K576, so these stars may be non-members. Another group of five BD stars [BD–134909 (181), BD–134913 (182), BD–144967 (183), BD–144972 (184), BD–144981 (186)] have $E(B-V) < 0.4$ mag and are located well above the birth-line, therefore these stars also could be non-members. The stars W483 (174) and K556 (176) occupy positions away from the MS. The former is just evolving off the MS and is probably a member while the latter may be affected by binarity. Star W483 with Hβ filled-in with emission and a candidate for a classical Be star is therefore more likely to be a cluster member. Stars BD–134909 (180) and BD–144994 (187), both of B-type, are quite interesting and are members as indicated from their PM, $E(B-V)$, R_V and HR diagram location; however, these are located diagonally ∼20 arcmin away from the cluster centre. The projected corona radius for the cluster is ∼15 arcmin (Belikov et al. 1999). Therefore if these are members then they probably formed in the outer region. Their location also indicates that the region of cluster formation would have been quite extended. Further

kinematical data is required to authenticate these possibilities. Among remaining objects, stars W235 (160), W469 (173) and W503 (175) have HAB characteristics. Star W235 has a value of $s \sim -2.3$, near blackbody and shows no intrinsic polarization (Orsatti, Vega & Marraco 2000), therefore it is probably a Group III HAB or a classical Be star. Star W503 has $s \sim -0.47$ and shows strong intrinsic polarization suggesting it to be a Group I HAB star. The stars W161 (154), W175 (155), W306 (166), W412 (171), W468 (172) and K601 (179) show MIR excesses, stars W175 and W412 are reported to be spectroscopic binary (Bosch, Morrell & Niemelaö 1999) while stars W175 and W306 show intrinsic polarization (Orsatti et al. 2000). Therefore all these stars appear to have circumstellar material and the stars W161, W306 and W468 are probably Vega-like.

NGC 6823 has an age ∼3 Myr and an age spread ∼9 Myr (Guetter 1992; Pigulski et al. 2000). A recent study by Pigulski et al. (2000) indicates that the stars with spectral classes later than A0 are in their PMS phase. Stars E36 (194), E78 (199), E92 (206), E96 (208), E103 (209) and E110 (211) are non-members, stars E92 and E96 have PM membership <0.5 while others lie above the birth-line. The spectrum obtained by us indicates that star E103 is a late A-type star, though it is reported to be of G8-type by Shi & Hu (1999). The remaining stars, 18 in total, are cluster members. Star E46 (195) occupies a position slightly away from the MS and is reported to show light variability. It is either a binary or a single star about to leave the MS. Of these, stars E4 (188), E80 (200), E84 (203) and E86 (204) have circumstellar material as indicated from MIR spectral indices. The value of *s* for star E104 (210) is above zero and it is a probable candidate Vega-like star. Star E4 has recently been argued to be a hot post-AGB candidate (Gauba et al. 2003) based on its IR excess, but, being a PM member, this is unlikely to be in a post-AGB phase.

6.2 Stars

Membership indicators suggest that the sample contains 34 non-members and 10 probable members while the remaining are members. These are indicated in the last column of Table 6. Around 16 per cent of the PM members were found to be non-members in the present study and this is supported in a few cases by recent PM studies. The converse is also true in a few cases, for example star 6 is a PM non-member, but other indicators suggest it to be a bona-fide member. Out of the total 28 identified emission-line stars, only 13 are of early type. Their characteristics suggest that they belong to the classical Be, Herbig Ae/Be or T Tauri populations. A group of 36 stars is reported to have weak to strong NIR excesses (29 members, five probable members and two non-members). Most of these are observed to be PMS objects. Another group of six stars (all members except one), show IR deficits. A group of 37 non-emission stars was identified to have circumstellar material as seen either from weak NIR excesses or MIR spectral indices. Of these, 25 (17 have above-zero values of *s* and eight have weak NIR excesses) are Vega-like or precursors to such stars (see Table 12) – one of these stars (13) has recently been shown to have Vega-like characteristics by Manoj et al. (2002). Three of these stars (87, 149, 151) are probably in a highly evolved stage with ages ∼20–30 Myr and with masses ∼10 –12 $M_{\odot}$.

7 CONCLUSIONS

We present the spectral and reddening properties of 211 highly reddened proper-motion members (mostly early type with $V < 15$ mag) in six young galactic clusters. The main conclusions of the study are given below.

(i) Emission features in Ca II HK and H I lines are observed for a sample of 29 stars including 11 reported for the first time. We also provide either a new or more reliable spectral class for a sample of 24 stars. Ca II triplet width measurements were used to indicate the presence of discs for a dozen stars; a few of them were found to be candidate weak-line T Tauri stars.

(ii) A significant fraction (>70 per cent) of cluster members in NGC 1976, NGC 2244, NGC 6530 and NGC 6611 show anomalous reddening with $R_V = 4.78 \pm 0.10$, 3.54 ± 0.04, 3.87 ± 0.05 and 3.56 ± 0.02, respectively, indicating the presence of larger grain-size dust in these star-forming regions. A small number of stars in NGC 1976, NGC 2244 and NGC 6611 also show normal behaviour while the cluster NGC 6823 appears to have normal reddening.

(iii) On the basis of spectral features, NIR excesses, dereddened colour–colour diagrams and MIR spectral indices we identify a highly probable group of five Herbig Ae/Be and six classical T Tauri stars. Moreover, a further probable group of three classical Be, five Herbig Ae/Be and nine weak-line T Tauri stars is also identified. These PMS population amounts to ∼15 per cent of the cluster members.

(iv) A total of 37 non-emission-line stars, mostly of early type, were identified to have circumstellar material as seen from weak NIR excesses or MIR spectral indices. Of these, 25 or 10 per cent of the early-type MS members appear to show Vega-like characteristics or are precursors to such a phenomenon.

(v) Three highly luminous late-type giants in two of the six clusters appear to be members and are in the post-hydrogen-core-burning stage, suggesting a prolonged duration (∼25 Myr) of star formation in these clusters.

ACKNOWLEDGMENTS

We gratefully acknowledge the valuable comments and suggestions given by an anonymous referee. We are grateful to Mount Stromlo Observatory, Australia for generous allotment of observing time. One of us (RS) is grateful to the IAU and the Anglo-Australian Observatory, Epping, Australia, for financial support during the observations. We are thankful to Dr A. K. Pandey for useful discussions. The data on PMS birth-lines were kindly provided by Francesco Palla. The present research makes use of data from: (i) the open cluster data base at the Web site http://obswww.unige.ch/webda/ maintained by Dr J. C. Mermilliod; (ii) 2-Micron All Sky Survey, which is a joint project of the University of Massachusetts and the Infrared Processing and Analysis Centre/California Institute of Technology, funded by the National Aeronautics and Space Administration and the National Science Foundation; (iii) the SIMBAD data base operated at CDS Strasbourg, France

REFERENCES

Beichman C., Neugebauer G., Habing H. J., Clegg P. E., Chester T. J., 1988, in NASA RP-1190, Vol. 1, IRAS Catalogs and Atlases Explanatory Supplement. GPO, Washington, DC

Belikov A. N., Kharchenko N. V., Piskunov A. E., Schilbach E., 1999, A&AS, 134, 525

Belikov A. N., Kharchenko N. V., Piskunov A. E., Schilbach E., 2000, A&A, 358, 886

Berghöfer T. W., Christian D. J., 2002, A&A, 384, 890

Bessell M. S., 1979, PASP, 91, 589

Bessell M. S., 1999, PASP, 111, 1426

Bessell M. S., Brett J. M., 1988, PASP, 100, 1134
Boesono B., Thé P. S., Tjin A Dijie H. R. E., 1987, Ap&SS, 137 167
Boggs D., Böhm-Vitense E., 1989, ApJ, 339, 209
Bohlin R. C., Savage B. D., 1981, ApJ, 249, 109
Bosch G. L., Morrell N. I., Niemelaö V. S., 1999, Rev. Mex. Astron. Astrofis., 35, 85
Cardelli J. A., Clayton G. C., Mathis J. A., 1989, ApJ, 345, 245
Carpenter J. M., 2001, AJ, 121, 2851
Chini R., Wargau W. F., 1990, A&A, 227, 213
Code A. D., Bless R. C., Davis J., Brown R. H., 1976, ApJ, 203, 417
Cutri R. M., 1998, BAAS 30, No. 2, 64.02
Danks A. C., Dennefeld M., 1994, PASP, 106, 382
D'Antona F., Mazzitelli I., 1994, ApJS, 90, 467
Elmegreen B. G., Lada C. J., 1977, AJ, 214, 725
Erickson R. R., 1971, A&A, 10, 270
FitzGerald M. P., 1970, A&A, 4, 234
Flaccomio E., Micela G., Sciortino S., Favata F., Corbally C., Tomaney A., 1999, A&A, 345, 521
Gauba G., Parthasarathy M., Kumar B., Yadav R. K. S., Sagar R., 2003, A&A, 404, 305
Greenstein J. L., Struve O., 1946, PASP, 58, 366
Guetter H. H., 1992, AJ, 103, 197
Gullbring E., Hartmann L., Briceno C., Calvet N., 1998, ApJ, 492, 323
Hartigan P., Strom K. M., Strom S. E., 1994, ApJ, 427, 961
He L., Whittet D. C. B., Kilkenny D., Spencer Jones J. H., 1995, ApJ, 101, 335
Herbig G. H., 1994, in Thé P. S., Pérez M. R., van den Heuvel P. J., eds, ASP Conf. Ser. Vol. 62, The Nature and Evolutionary Status of Herbig Ae/Be Stars. Astron. Soc. Pac., San Francisco, p. 3
Hillenbrand L. A., 1997, AJ, 113, 1733
Hillenbrand L. A., 2002, preprint (astro-ph/0210520)
Hillenbrand L. A., Strom S. E., Vrba F. J., Kenne J., 1992, ApJ, 397, 613
Hillenbrand L. A., Massey P., Strom S. E., Merrill K. M., 1993, AJ, 106, 1906
Hillenbrand L. A., Strom S. E., Calvet N., Merrill K. M., Gatley I., Makidon R. B., Meyer M. R., Skrutskie M. E., 1998, AJ, 116, 1816
Hiltner W. A., Morgan W. W., Neff J. S., 1965, ApJ, 141, 183
Jacoby G. H., Hunter D. A., Christian C. A., 1984, ApJS, 56, 257
Jaschek C., Jaschek M., 1987, The Classification of Stars. Cambridge Univ. Press, Cambridge
Johnson H. L., 1966, ARA&A, 4, 193
Johnson H. L., 1967, ApJ, 150, 39
Johnson H. L., 1968, in Middlehurst B. M., Aller L. H., eds, Stars and Stellar Systems, Vol. 7, Nebulae and Interstellar Matter. Univ. Chicago Press, Chicago
Johnson H. M., 1965, ApJ, 142, 964
Kamp L. W., 1974, A&AS, 16, 1
Keller S. C., 1999, AJ, 118, 889
Keller S. C., Bessell M. S., Da Costa G. S., 2000, AJ, 119, 1748
Kippenhahn R., 1965, Veroeffentlichungen der Remeis-Sternwarte zu Bamberg, Nr. 40, 7
Koornneef J., 1983, A&A, 128, 84
Krełowski J., Strobel A., 1979, Acta Astron., 29, 211
Krełowski J., Strobel A., 1987, A&A, 175, 186
Kurucz R. L., 1993, CD-ROM No. 13
LaSala J., Kurtz M. J., 1985, PASP, 97, 605
Leinert C., Richichi A., Haas M., 1997, A&A, 318, 472
Levato H., Abt H. A., 1976, PASP, 88, 712
Littlefair S. P., Naylor T., Harries T. J., 2004, MNRAS, 347, 937
McNamara B. J., Huels S., 1983, A&AS, 54, 221
Maheswar G., Manoj P., Bhatt H. C., 2002, A&A, 387, 1003
Manoj P., Maheswar G., Bhatt H. C., 2002, MNRAS, 334, 419
Margulis M., Lada C. J., 1984, Occ. Rep. R. Obs. Edin., No. 13, 41
Marschall L. A., van Altena W. F., Chiu L. T. C., 1982, AJ, 87, 1497
Martin P. G., Whittet D. C. B., 1990, ApJ, 357, 113
Massa D., Conti P. S., 1981, ApJ, 248, 201
Massey P., Parker J. W., Garmany G. D., 1989, AJ, 98, 1305
Massey P., Johnson K. E., DeGioia-Eastwood K., 1995, ApJ, 454, 151
Mathis J. S., 1990, ARA&A, 28, 37
Meeus G., Waters L. B. F. M., Bouwman J., van den Ancker M. E., Waelkens C., Malfait K., 2001, A&A, 365, 476
Mendez M. E., 1967, Bol. Obs. Tonantzintla y Tacubaya, 4, 91
Mendoza V. E. E., Gömez T., 1980, MNRAS, 190, 623
Mermilliod J.-C., Paunzen E., 2003, A&A, 410, 511
Meyer M. R., Calvet N., Hillenbrand L. A., 1997, AJ, 114, 288
Ogura K., Ishida K., 1981, PASJ, 33, 149
Omont A. et al., 2003, A&A, 403, 975
Orsatti A. M., Vega E. I., Marraco H. G., 2000, A&AS, 144, 195
Palla F., Stahler S. W., 1993, ApJ, 418, 414
Pandey A. K., Mahra H. S., Sagar R., 1990, AJ, 99, 617
Pandey A. K., Upadhyay K., Nakada Y., Ogura K., 2003, A&A, 388, 158
Panek R. J., 1983, ApJ, 270, 169
Parenago P. P., 1954, Catalogue of Stars in the Area of the Orion Nebula, Trudy Sternberg Astron. Inst. Vol. 25
Park B.-G., Sung H., 2002, AJ, 123, 892
Park B.-G., Sung H., Bessell M. S., Kang Y. H., 2000, AJ, 120, 894
Park B.-G., Sung H., Kang Y. H., 2002, J. Korean Astron. Soc. 35, 197
Pérez M. R., 1991, Rev. Mex. Astron. Astrofis 22, 99
Pérez M. R., Thé P. S., Westerlund B. E., 1987, PASP, 99, 1050
Pigulski A., Kolaczkowski Z., Kopacki G., 2000, Acta Astron. 50, 113
Price S. D., Egan M. P., Carey S. J., Mizuno D. R., Kuchar T. A., 2001, AJ, 121, 2819
Qian Z. Y., Sagar R., 1994, MNRAS, 266, 114
Rebull L. M. et al., 2002, AJ, 123, 1528
Rieke G. H., Lebofsky M. J., 1985, ApJ, 288, 618
Sabogal-Martínez B. E., García-Varela M. A., Higuera G., Uribe A., Brieva E., 2001, Rev. Mex. Astron. Astrofis., 37, 105
Sagar R., 1987, MNRAS, 228, 483
Sagar R., Joshi U. C., 1978, MNRAS, 184, 467
Sagar R., Joshi U. C., 1979, A&AS, 66, 3
Sagar R., Joshi U. C., 1981, Ap&SS, 75, 465
Sagar R., Joshi U. C., 1983, MNRAS, 205, 747
Sagar R., Qian Z. Y., 1993, Bull. Astron. Soc. India, 21, 565
Schaller G., Schaerer D., Meynet G., Maerder A., 1992, A&AS, 96, 269
Schmidt-Kaler Th., 1982, Landolt Börstein Catalogue, Vol. VI/2b
Schuller F. et al., 2003, A&A, 403, 955
Shi H. M., Hu J. Y., 1999, A&AS, 136, 313
Skrutskie M. F. et al., 1997, in Garzon F., Epchtein N., Omont A., Burton B., Persi P., eds, The Impact of Large Scale Near-IR Sky Surveys. Kluwer, Dordrecht, p. 25
Sung H., Bessell M. S., Lee S. W., 1997, AJ, 114, 2644
Sung H., Chun M.-Y., Bessell M. S., 2000, AJ, 120, 333
Terranegra L., Chavarria-K C., Diaz S., González-Patiño D., 1994, A&AS, 104, 557
Tian K. P., van Leeuwen Zhao, J. L., Su C. G., 1996, A&AS, 118, 503
Tonry J., Davis M., 1979, AJ, 84, 1511
Torres A. V., 1987, ApJ, 322, 949
Vasilevskis S., Sanders W. L., Balz A. C. A., Jr, 1965, AJ, 70, 797
van Altena W. F., Jones B. F., 1972, A&A, 20, 425
van den Ancker M. E., Thé P. S., Feinstein A., Vázquez R. A., de Winter D., Pérez M. R., 1997, A&AS, 123, 63
Walker M. F., 1956, ApJS, 2, 365
Walker M. F., 1957, ApJ, 125, 636
Walker M. F., 1961, ApJ, 133, 438
Walker M. F., 1969, ApJ, 155, 447
Whittet D. C. B., van Breda I. G., 1980, MNRAS, 192, 467
Wolff S. C., Strom S. E., Hillenbrand L. A., 2004, ApJ, 601, 979
Wood P. R., Bessell M. S., Fox M. W., 1983, ApJ, 272, 99
Yadav R. K. S., Sagar R., 2002, MNRAS, 337, 133

This paper has been typeset from a TEX/LATEX file prepared by the author.